Tanaka N, Moriya K, Kiyosawa K, Koike K, Aoyama T.	Hepatitis C virus core protein induces spontaneous and persistent activation of peroxisome proliferator-activated receptor alpha in transgenic mice: Implications for HCV-associated hepatocarcinogenesis.	Int J Cancer	122	124-31	2008
Koike K, Kikuchi Y, Kato M, Takamatsu J, Shintani Y, Tsutsumi T, Fujie H, Miyoshi H, Moriya K, Yotsuyanagi H.	Prevalence of Hepatitis B Virus Infection in Patients with Human Immunodeficiency Virus in Japan.	Hep Res	38	310-314	2008
Nagase Y, Yotsuyanagi H, Okuse C, Yasuda K, Kato T, Koike K, Suzuki M, Nishioka K, Iino S, Itoh F.	Effect of treatment with interferon alpha-2b and ribavirin in patients infected with genotype 2 hepatitis C virus.	Hepatol Res	38	252-258	2008
Koike K, Tsutsumi T, Miyoshi H, Shinzawa S, Shintani Y, Fujie H, Yotsuyanagi H, Moriya K.	Molecular Basis for the Synergy between Alcohol and Hepatitis C Virus in Hepatocarcinogenesis.	J Gastroenterol Hepatol	23	S87-91	2008
Newell P, Villanueva A, Friedman SL, Koike K, Llovet JM.	Experimental models of hepatocellular carcinoma.	J Hepatol	48	858-879	2008;
Ishizaka N, Ishizaka Y, Seki G, Nagai R, Yamakado M, Koike K.	Association between hepatitis B/C viral infection, chronic kidney disease and insulin resistance in individuals undergoing general health screening.	Hepatol Res	38	775-783.	2008
Seya, T., and M. Matsumoto	The extrinsic RNA-sensing pathway for adju- vant immunotherapy of cancer.	Cancer Immu. Immunother.		In press	2009
S eya, T., M. Matsumoto, T.	Functional evolution of the TICAM-1 pathway	Immunol. Reviews	227	44-53	2009

Ebihara, and H. Oshiumi.	for extrinsic RNA sensing.				
Oshiumi, H., M. Matsumoto, S. Hatake-yama, and T. Seya.	Riplet/RNF135, a RING-finger protein, ubiquitinates RIG-I to promote interferon-b induction during the early phase of viral infection.	J. Biol. Chem.	284	807-817	2009
Itoh K., A. Watanabe, K. Funami, T. Seya, and M. Matsumoto	The clathrin-mediated endocytic pathway participates in dsRNA-induced IFN-b production.	J. Immunol.	181	5522-5529	2008
Matsuo A., H. Oshiumi, M. Matsumoto, T. Seya et al.	Teleost Toll-like receptor 22 recognizes RNA duplex to induce IFN and protect cells from Bir- naviruses.	.J. Immunol.	181	3474-3485	2008
Shingai, M., T. Ebihara, M. Matsumoto, T. Seya et al.	Soluble G protein of respiratory syncytial virus inhibits Toll-like rceptor 3/4-mediated interferon-beta induction.	Int. I2008mmunol.	20	1169-118	2008
Oshiumi, H., A. Matsuo, M. Matsumoto, and T. Seya	Pan-Vertebrate Toll-like receptors during evolution.	Current Genomics	9	488-493	2008
Fukuda, K., T. Watanabe, T. Seya, M. Matsumoto et al.	Modulation of double-stranded RNA recognition by the N-terminal histidine-rich region of the human Toll-like Receptor 3.	J. Biol. Chem.	283	22784-227 94	2008
Funami, K., M. Sasai, H. Oshiumi, T. Seya, and M. Matsumoto.	Homo-oligomerization is essential for Toll/IL-1 receptor domain-containing adaptor mole- cule-1 mediated NF-kB and IRF-3 acti- vation.	J. Biol. Chem.	283	18283-182 91	2008

Nakamura, M., K. Funami, M. Matsumoto, T. Seya et al.,	Increased expression of Toll-like receptor 3 in intrahepatic bilinary epithelial cells at sites of ductular reaction in diseased livers.	Hepatol. Int.	2:	222-230	2008
Shime, H., M. Yabu, T. Akazawa, K. Kodama, M. Matsumoto, T. Seya and N. Inoue.	Tumor-secreted lactic acid promotes IL-23-IL-17 proinflammatory pathway.	J. Immunol.	180	7175-7183	2008
Seya, T	Preface	ADDR	60	779-781	2008
Matsumoto M., and T. Seya	TLR3: Interferon induction by double-stranded RNA including poly(I:C).	ADD	60	805-812	2008
Ebihara, T., M. Shingai, M. Matsumoto, T. Wakita, and T. Seya.	Hepatitis Cvirus (HCV)-infected apoptotic cells extrinsically modulate dendritic cell function to activate T cells and NK cells	Hepatology	48	48-58	2008
Bas, S., T. Seya, M, Matsumoto et al.	The pro-inflammatory cytokine response to Chlamydia trachomatis elementary bodies in human macrophages is partly mediated by a lipoprotein, the macrophage infectivity potentiator, through TLR2/TLR1/TLR6 and CD14.	J. Immunol.	180	1158-1168	2008
Oshiumi, H., T. Seya, M. Matsumoto, et al.	Pan-vertebrate Toll-like receptors during evolution.	Cur. Genomics	9	In press	2008
Wu, J. D., T. Seya, M. Matsumoto, et al.	Obstructing Shedding of the immunostimulatory MHC class I chain-related gene B prevents tumor formation.	Clin. Cancer Res.	15	632-639	2009

Ⅳ．研究成果の刊行物・別刷

zjv00509/zjv157709z | xppws | S=1 | 1/6/09 | Art: 1690-08
zjs / DOCHEAD=NOTE zjss / DOCTOPIC=VIRUS-CELL INTERACTIONS
FROM COVER SHEET: Editor: Perlman Article No.: N Section: Interactions

JOURNAL OF VIROLOGY, Mar. 2009, p. 000 Vol. 83, No. 5
0022-538X/09/$08.00+0 doi:10.1128/JVI.01690-08

Proteasomal Turnover of Hepatitis C Virus Core Protein Is Regulated by Two Distinct Mechanisms: a Ubiquitin-Dependent Mechanism and a Ubiquitin-Independent but PA28γ-Dependent Mechanism▽

Ryosuke Suzuki,[1] Kohji Moriishi,[2] Kouichirou Fukuda,[1] Masayuki Shirakura,[1] Koji Ishii,[1] Ikuo Shoji,[3] Takaji Wakita,[1] Tatsuo Miyamura,[1] Yoshiharu Matsuura,[2] and Tetsuro Suzuki[1]*

Department of Virology II, National Institute of Infectious Diseases, Tokyo 162-8640,[1] Department of Molecular Virology, Research Institute for Microbial Diseases, Osaka University, Osaka 565-0871,[2] and Division of Microbiology, Kobe University Graduate School of Medicine, Hyogo 650-0017,[3] Japan

Received 8 August 2008/Accepted 5 December 2008

We have previously reported on the ubiquitylation and degradation of hepatitis C virus core protein. Here we demonstrate that proteasomal degradation of the core protein is mediated by two distinct mechanisms. One leads to polyubiquitylation, in which lysine residues in the N-terminal region are preferential ubiquitylation sites. The other is independent of the presence of ubiquitin. Gain- and loss-of-function analyses using lysineless mutants substantiate the hypothesis that the proteasome activator PA28γ, a binding partner of the core, is involved in the ubiquitin-independent degradation of the core protein. Our results suggest that turnover of this multifunctional viral protein can be tightly controlled via dual ubiquitin-dependent and -independent proteasomal pathways.

Fn1 Hepatitis C virus (HCV) core protein, whose amino acid sequence is highly conserved among different HCV strains, not only is involved in the formation of the HCV virion but also has a number of regulatory functions, including modulation of signaling pathways, cellular and viral gene expression, cell transformation, apoptosis, and lipid metabolism (reviewed in references 9 and 15). We have previously reported that the E6AP E3 ubiquitin (Ub) ligase binds to the core protein and plays an important role in polyubiquitylation and proteasomal degradation of the core protein (22). Another study from our group identified the proteasome activator PA28γ/REG-γ as an HCV core-binding partner, demonstrating degradation of the core protein via a PA28γ-dependent pathway (16, 17). In this work, we further investigated the molecular mechanisms underlying proteasomal degradation of the core protein and found that in addition to regulation by the Ub-mediated pathway, the turnover of the core protein is also regulated by PA28γ in a Ub-independent manner.

Although ubiquitylation of substrates generally requires at least one Lys residue to serve as a Ub acceptor site (5), there is no consensus as to the specificity of the Lys targeted by Ub (4, 8). To determine the sites of Ub conjugation in the core protein, we used site-directed mutagenesis to replace individual Lys residues or clusters of Lys residues with Arg residues in the N-terminal 152 amino acids (aa) of the core (C152), within F1 which is contained all seven Lys residues (Fig. 1A). Plasmids expressing a variety of mutated core proteins were generated by PCR and inserted into the pCAGGS (18). Each core-expressing construct was transfected into human embryonic kidney 293T cells along with the pMT107 (25) encoding a Ub moiety tagged with six His residues (His_6). Transfected cells were treated with the proteasome inhibitor MG132 for 14 h to maximize the level of Ub-conjugated core intermediates by blocking the proteasome pathway and were harvested 48 h posttransfection. His_6-tagged proteins were purified from the extracts by Ni^{2+}-chelation chromatography. Eluted protein and whole lysates of transfected cells before purification were analyzed by Western blotting using anticore antibodies (Fig. 1B). Mutations replacing one or two Lys residues with Arg in the core protein did not affect the efficiency of ubiquitylation: detection of multiple Ub-conjugated core intermediates was observed in the mutant core proteins comparable to the results seen with the wild-type core protein as previously reported (23). In contrast, a substitution of four N-terminal Lys residues (C152K6 to -23R) caused a significant reduction in ubiquitylation (Fig. 1B, lane 9). Multiple Ub-conjugated core intermediates were not detected in the Lys-less mutant (C152KR), in which all seven Lys residues were replaced with Arg (Fig. 1B, lane 11). These results suggest that there is not a particular Lys residue in the core protein to act as the Ub acceptor but that more than one Lys located in its N-terminal region can serve as the preferential ubiquitylation site. In rare cases, Ub is known to be conjugated to the N terminus of proteins; however, these results indicate that this does not occur within the core protein.

To investigate how polyubiquitylation correlates with proteasome degradation of the core protein, we performed kinetic analysis of the wild-type and mutated core proteins by use of the Ub protein reference (UPR) technique, which can compensate for data scatter of sample-to-sample variations such as levels of expression (10, 24). Fusion proteins expressed from UPR-based constructs (Fig. 2A) were cotranslationally cleaved F2 by deubiquitylating enzymes, thereby generating equimolar quantities of the core proteins and the reference protein, dihydrofolate reductase-hemagglutinin (DHFR-HA) tag-modified Ub, in which the Lys at aa 48 was replaced by Arg to prevent its polyubiquitylation (Ub^{R48}). After 24 h of transfec-

* Corresponding author. Mailing address: Department of Virology II, National Institute of Infectious Diseases, 1-23-1 Toyama, Shinjuku-ku, Tokyo 162-8640, Japan. Phone: 81-3-5285-1111. Fax: 81-3-5285-1161. E-mail: tesuzuki@nih.go.jp.

▽ Published ahead of print on 17 December 2008.

zjv00509/zjv157709z | xppws | S=1 | 1/6/09 | Art: 1690-08

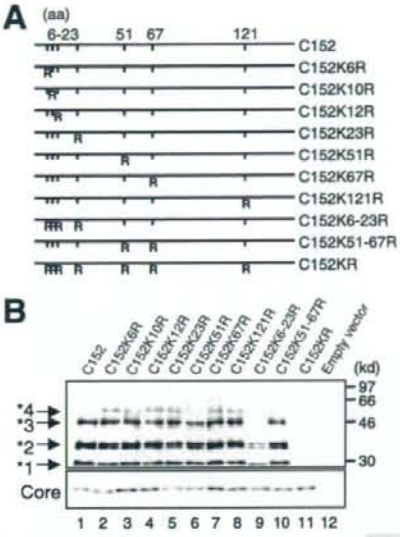

FIG. 1. In vivo ubiquitylation of HCV core protein. (A) The HCV core protein (N-terminal 152 aa) is represented on the top. The positions of the amino acid residues of the core protein are indicated above the bold lines. The positions of the seven Lys residues in the core are marked by vertical ticks. Substitution of Lys with Arg (R) is schematically depicted. (B) Detection of ubiquitylated forms of the core proteins. The transfected cells with core expression plasmids and pMT107 were treated with the proteasome inhibitor MG132 and harvested 48 h after transfection. His_6-tagged proteins were purified and subsequently analyzed by Western blot analysis using anticore antibody (upper panel). Core proteins conjugated to a number of His_6-Ub are denoted with asterisks. Whole lysates of transfected cells before purification were also analyzed (lower panel). Lanes 1 to 11, C152 to C152KR, as indicated for panel A. Lane 12; empty vector.

AQ: A

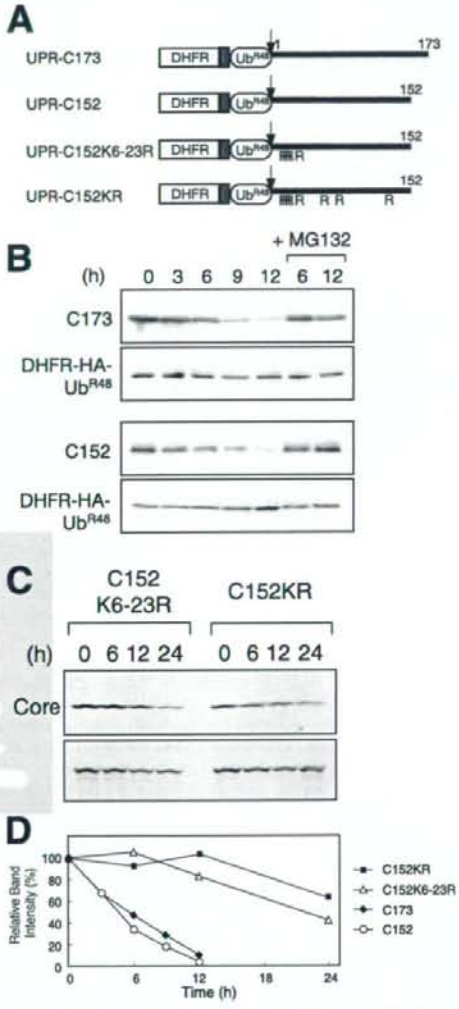

FIG. 2. Kinetic analysis of degradation of HCV core proteins. (A) The fusion constructs used in the UPR technique. Open boxes indicate the DHFR sequence, which is extended at the C terminus by a sequence containing the HA epitope (hatched boxes). Ub^{R48} moieties bearing the Lys-Arg substitution at aa 48 are represented by open ellipses. Bold lines indicate the regions of the core protein. The amino acid positions of the core protein are indicated above the bold lines. The arrows indicate the sites of in vivo cleavage by deubiquitylating enzymes. (B and C) Turnover of the core proteins. After a 24-h transfection with each UPR construct, cells were treated with 50 μg of cycloheximide/ml in the presence or absence of 10 μM MG132 for the different time periods indicated. Cells were lysed at the different time points indicated, followed by evaluation via sodium dodecyl sulfate-polyacrylamide gel electrophoresis and Western blot analysis using antibodies against the core protein and HA. (D) Quantitation of the data shown in panels B and C. At each time point, the ratio of band intensity of the core protein relative to the reference DHFR-HA-Ub^{R48} was determined by densitometry and is plotted as a percentage of the ratio at time zero.

tion with UPR constructs, cells were treated with cycloheximide and the amounts of core proteins and DHFR-HA-Ub^{R48} at the indicated time points were determined by Western blot analysis using anticore and anti-HA antibodies. The mature form of the core protein, aa 1 to 173 (C173) (13, 20), and C152 were degraded with first-order kinetics (Fig. 2B and D). MG132 completely blocked the degradation of C173 and C152 (Fig. 2B), and C152K6-23R and C152KR were markedly stabilized (Fig. 2C). The half-lives of C173 and C152 were calculated to be 5 to 6 h, whereas those of C152K6-23R and C152KR were calculated to be 22 to 24 h (Fig. 2D), confirming that the Ub plays an important role in regulating degradation of the core protein. Nevertheless, these results also suggest possible involvement of the Ub-independent pathway in the turnover of the core protein, as C152KR is more destabilized than the reference protein (Fig. 2C and 2D).

We have shown that PA28γ specifically binds to the core protein and is involved in its degradation (16, 17). Recent studies demonstrated that PA28γ is responsible for Ub-independent degradation of the steroid receptor coactivator SRC-3 and cell cycle inhibitors such as p21 (3, 11, 12). Thus, we next investigated the possibility of PA28γ involvement in the deg-

zjv00509/zjv157709z | xppws | S=1 | 1/6/09 | Art: 1690-08

radation of either C152KR or C152. Since C152KR carries two amino acid substitutions in the PA28γ-binding region (aa 44 to 71) (17), we tested the influence of the mutations of C152KR on the interaction with PA28γ by use of a coimmunoprecipitation assay. When Flag-tagged PA28γ (F-PA28γ) was expressed in cells along with C152 or C152KR, F-PA28γ precipitated along with both C152 and C152KR, indicating that PA28γ interacts with both core proteins (Fig. 3A). Figure 3B reveals the effect of exogenous expression of F-PA28γ on the steady-state levels of C152 and C152KR. Consistent with previous data (17), the expression level of C152 was decreased to a nearly undetectable level in the presence of PA28γ (Fig. 3B, lanes 1 and 3). Interestingly, exogenous expression of PA28γ led to a marked reduction in the amount of C152KR expressed (Fig. 3B, lanes 5 and 7). Treatment with MG132 increased the steady-state level of the C152KR in the presence of F-PA28γ as well as the level of C152 (Fig. 3B, lanes 4 and 8).

We further investigated whether PA28γ affects the turnover of Lys-less core protein through time course experiments. C152KR was rapidly destabilized and almost completely degraded in a 3-h chase experiment using cells overexpressing F-PA28γ (Fig. 3C, left panels). A similar result was obtained using an analogous Lys-less mutant of the full-length core protein C191KR (Fig. 3C, right panels), thus demonstrating that the Lys-less core protein undergoes proteasomal degradation in a PA28γ-dependent manner. These results suggest that PA28γ may play a role in accelerating the turnover of the HCV core protein that is independent of ubiquitylation.

Finally, we examined gain- and loss-of-function of PA28γ with respect to degradation of full-length wild-type (C191) and mutated (C191KR) core proteins in human hepatoma Huh-7 cells. As expected, exogenous expression of PA28γ or E6AP caused a decrease in the C191 steady-state levels (Fig. 4A). In contrast, the C191KR level was decreased with expression of PA28γ but not of E6AP. We further used RNA interference to inhibit expression of PA28γ or E6AP. An increase in the abundance of C191KR was observed with PA28γ small interfering RNA (siRNA) but not with E6AP siRNA (Fig. 4B). An increase in the C191 level caused by the activity of siRNA against PA28γ or E6AP was confirmed as well.

Taking these results together, we conclude that turnover of the core protein is regulated by both Ub-dependent and Ub-independent pathways and that PA28γ is possibly involved in Ub-independent proteasomal degradation of the core protein. PA28 is known to specifically bind and activate the 20S proteasome (19). Thus, PA28γ may function by facilitating the delivery of the core protein to the proteasome in a Ub-independent manner.

Accumulating evidence suggests the existence of proteasome-dependent but Ub-independent pathways for protein degradation, and several important molecules, such as p53, p73, Rb, SRC-3, and the hepatitis B virus X protein, have two distinct degradation pathways that function in a Ub-dependent and Ub-independent manner (1, 2, 6, 7, 14, 21, 27). Recently, critical roles for PA28γ in the Ub-independent pathway have been demonstrated; SRC-3 and p21 can be recognized by the 20S proteasome independently of ubiquitylation through their interaction with PA28γ (3, 11, 12). It has also been reported that phosphorylation-dependent ubiquitylation mediated by GSK3 and SCF is important for SRC-3 turnover (26). Never-

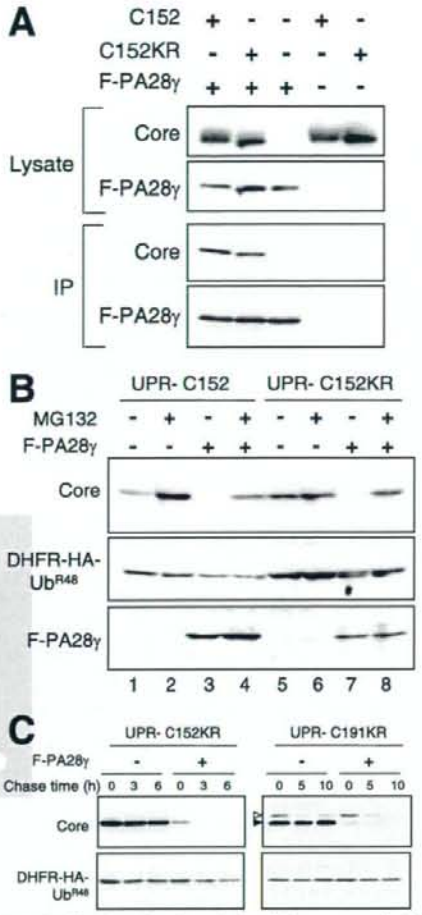

FIG. 3. PA28γ-dependent degradation of the core protein. (A) Interaction of the core protein with PA28γ. Cells were cotransfected with the wild-type (C152) or Lys-less (C152KR) core expression plasmid in the presence of a Flag-PA28γ (F-PA28γ) expression plasmid or an empty vector. The transfected cells were treated with MG132. After 48 h, the cell lysates were immunoprecipitated with anti-Flag antibody and visualized by Western blotting with anticore antibodies. Western blot analysis of whole cell lysates was also performed. (B) Degradation of the wild-type and Lys-less core proteins via the PA28γ-dependent pathway. Cells were transfected with the UPR construct with or without F-PA28γ. In some cases, cells were treated with 10 μM MG132 for 14 h before harvesting. Western blot analysis was performed using anticore, anti-HA, and anti-Flag antibodies. (C) After 24 h of transfection with UPR-C152KR and UPR-C191KR with or without F-PA28γ (an empty vector), cells were treated with 50 μg of cycloheximide/ml for different time periods as indicated (chase time). Western blot analysis was performed using anticore and anti-HA antibodies. The precursor core protein and the core that was processed, presumably by signal peptide peptidase, are denoted by open and closed triangles, respectively.

zjv00509/zjv157709z | xppws | S=1 | 1/6/09 | Art: 1690-08

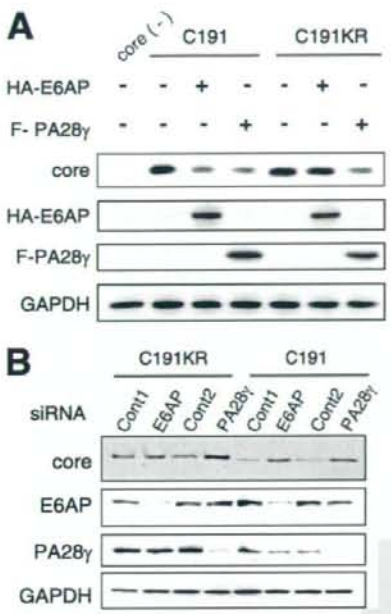

FIG. 4. Ub-dependent and Ub-independent degradation of the full-length core protein in hepatic cells. (A) Huh-7 cells were cotransfected with plasmids for the full-length core protein (C191) or its Lys-less mutant (C191KR) in the presence of F-PA28γ or HA-tagged-E6AP expression plasmid (HA-E6AP). After 48 h, cells were lysed and Western blot analysis was performed using anticore, anti-HA, anti-Flag, or anti-GAPDH. (B) Huh-7 cells were cotransfected with core expression plasmids along with siRNA against PA28γ or E6AP or against negative control siRNA. Cells were harvested 72 h after transfection and subjected to Western blot analysis.

theless, the precise mechanisms underlying turnover of most of the proteasome substrates that are regulated in both Ub-dependent and Ub-independent manners are not well understood. To our knowledge, the HCV core protein is the first viral protein studied that has led to identification of key cellular factors responsible for proteasomal degradation via dual distinct mechanisms. Although the question remains whether there is a physiological significance of the Ub-dependent and Ub-independent degradation of the core protein, it is reasonable to consider that tight control over cellular levels of the core protein, which is multifunctional and essential for viral replication, maturation, and pathogenesis, may play an important role in representing the potential for its functional activity.

This work was supported by a grant-in-aid for Scientific Research from the Japan Society for the Promotion of Science, from the Ministry of Health, Labor and Welfare of Japan, and from the Ministry of Education, Culture, Sports, Science and Technology, by Research on Health Sciences focusing on Drug Innovation from the Japan Health Sciences Foundation, Japan, and by the Program for Promotion of Fundamental Studies in Health Sciences of the National Institute of Biomedical Innovation of Japan.

REFERENCES

1. **Asher, G., J. Lotem, L. Sachs, C. Kahana, and Y. Shaul.** 2002. Mdm-2 and ubiquitin-independent p53 proteasomal degradation regulated by NQO1. Proc. Natl. Acad. Sci. USA **99:**13125–13130.
2. **Asher, G., P. Tsvetkov, C. Kahana, and Y. Shaul.** 2005. A mechanism of ubiquitin-independent proteasomal degradation of the tumor suppressors p53 and p73. Genes Dev. **19:**316–321.
3. **Chen, X., L. F. Barton, Y. Chi, B. E. Clurman, and J. M. Roberts.** 2007. Ubiquitin-independent degradation of cell-cycle inhibitors by the REGγ proteasome. Mol. Cell **26:**843–852.
4. **Ciechanover, A.** 1998. The ubiquitin-proteasome pathway: on protein death and cell life. EMBO J. **17:**7151–7160.
5. **Hershko, A., A. Ciechanover, and A. Varshavsky.** 2000. The ubiquitin system. Nat. Med. **6:**1073–1081.
6. **Jariel-Encontre, I., M. Pariat, F. Martin, S. Carillo, C. Salvat, and M. Piechaczyk.** 1995. Ubiquitinylation is not an absolute requirement for degradation of c-Jun protein by the 26 S proteasome. J. Biol. Chem. **270:**11623–11627.
7. **Jin, Y., H. Lee, S. X. Zeng, M. S. Dai, and H. Lu.** 2003. MDM2 promotes p21waf1/cip1 proteasomal turnover independently of ubiquitylation. EMBO J. **22:**6365–6377.
8. **Ju, D., and Y. Xie.** 2006. Identification of the preferential ubiquitination site and ubiquitin-dependent degradation signal of Rpn4. J. Biol. Chem. **281:**10657–10662.
9. **Lai, M. M. C., and C. F. Ware.** 1999. Hepatitis C virus core protein: possible roles in viral pathogenesis. Springer, Berlin, Germany.
10. **Lévy, F., N. Johnsson, T. Rumenapf, and A. Varshavsky.** 1996. Using ubiquitin to follow the metabolic fate of a protein. Proc. Natl. Acad. Sci. USA **93:**4907–4912.
11. **Li, X., L. Amazit, W. Long, D. M. Lonard, J. J. Monaco, and B. W. O'Malley.** 2007. Ubiquitin- and ATP-independent proteolytic turnover of p21 by the REGγ-proteasome pathway. Mol. Cell **26:**831–842.
12. **Li, X., D. M. Lonard, S. Y. Jung, A. Malovannaya, Q. Feng, J. Qin, S. Y. Tsai, M. J. Tsai, and B. W. O'Malley.** 2006. The SRC-3/AIB1 coactivator is degraded in a ubiquitin- and ATP-independent manner by the REGγ proteasome. Cell **124:**381–392.
13. **Liu, Q., C. Tackney, R. A. Bhat, A. M. Prince, and P. Zhang.** 1997. Regulated processing of hepatitis C virus core protein is linked to subcellular localization. J. Virol. **71:**657–662.
14. **Lonard, D. M., Z. Nawaz, C. L. Smith, and B. W. O'Malley.** 2000. The 26S proteasome is required for estrogen receptor-α and coactivator turnover and for efficient estrogen receptor-α transactivation. Mol. Cell **5:**939–948.
15. **Moradpour, D., F. Penin, and C. M. Rice.** 2007. Replication of hepatitis C virus. Nat. Rev. Microbiol. **5:**453–463.
16. **Moriishi, K., R. Mochizuki, K. Moriya, H. Miyamoto, Y. Mori, T. Abe, S. Murata, K. Tanaka, T. Miyamura, T. Suzuki, K. Koike, and Y. Matsuura.** 2007. Critical role of PA28γ in hepatitis C virus-associated steatogenesis and hepatocarcinogenesis. Proc. Natl. Acad. Sci. USA **104:**1661–1666.
17. **Moriishi, K., T. Okabayashi, K. Nakai, K. Moriya, K. Koike, S. Murata, T. Chiba, K. Tanaka, R. Suzuki, T. Suzuki, T. Miyamura, and Y. Matsuura.** 2003. Proteasome activator PA28γ-dependent nuclear retention and degradation of hepatitis C virus core protein. J. Virol. **77:**10237–10249.
18. **Niwa, H., K. Yamamura, and J. Miyazaki.** 1991. Efficient selection for high-expression transfectants with a novel eukaryotic vector. Gene **108:**193–199.
19. **Realini, C., C. C. Jensen, Z. Zhang, S. C. Johnston, J. R. Knowlton, C. P. Hill, and M. Rechsteiner.** 1997. Characterization of recombinant REGα, REGβ, and REGγ proteasome activators. J. Biol. Chem. **272:**25483–25492.
20. **Santolini, E., G. Migliaccio, and N. La Monica.** 1994. Biosynthesis and biochemical properties of the hepatitis C virus core protein. J. Virol. **68:**3631–3641.
21. **Sheaff, R. J., J. D. Singer, J. Swanger, M. Smitherman, J. M. Roberts, and B. E. Clurman.** 2000. Proteasomal turnover of p21Cip1 does not require p21Cip1 ubiquitination. Mol. Cell **5:**403–410.
22. **Shirakura, M., K. Murakami, T. Ichimura, R. Suzuki, T. Shimoji, K. Fukuda, K. Abe, S. Sato, M. Fukasawa, Y. Yamakawa, M. Nishijima, K. Moriishi, Y. Matsuura, T. Wakita, T. Suzuki, P. M. Howley, T. Miyamura, and I. Shoji.** 2007. E6AP ubiquitin ligase mediates ubiquitylation and degradation of hepatitis C virus core protein. J. Virol. **81:**1174–1185.
23. **Suzuki, R., K. Tamura, J. Li, K. Ishii, Y. Matsuura, T. Miyamura, and T. Suzuki.** 2001. Ubiquitin-mediated degradation of hepatitis C virus core protein is regulated by processing at its carboxyl terminus. Virology **280:**301–309.
24. **Suzuki, T., and A. Varshavsky.** 1999. Degradation signals in the lysine-asparagine sequence space. EMBO J. **18:**6017–6026.
25. **Treier, M., L. M. Staszewski, and D. Bohmann.** 1994. Ubiquitin-dependent c-Jun degradation in vivo is mediated by the δ domain. Cell **78:**787–798.
26. **Wu, R. C., Q. Feng, D. M. Lonard, and B. W. O'Malley.** 2007. SRC-3 coactivator functional lifetime is regulated by a phospho-dependent ubiquitin time clock. Cell **129:**1125–1140.
27. **Zhang, Z., and R. Zhang.** 2008. Proteasome activator PA28γ regulates p53 by enhancing its MDM2-mediated degradation. EMBO J. **27:**852–864.

Virology 383 (2009) 319–327

Contents lists available at ScienceDirect

Virology

journal homepage: www.elsevier.com/locate/yviro

Cellular vimentin content regulates the protein level of hepatitis C virus core protein and the hepatitis C virus production in cultured cells

Yuko Nitahara-Kasahara [a,1], Masayoshi Fukasawa [a,*], Fumiko Shinkai-Ouchi [a], Shigeko Sato [a], Tetsuro Suzuki [b], Kyoko Murakami [b], Takaji Wakita [b], Kentaro Hanada [a], Tatsuo Miyamura [c], Masahiro Nishijima [a,d]

[a] Department of Biochemistry and Cell Biology, National Institute of Infectious Diseases, 1-23-1, Toyama, Shinjuku-ku, Tokyo 162-8640, Japan
[b] Department of Virology II, National Institute of Infectious Diseases, Tokyo 162-8640, Japan
[c] National Institute of Infectious Diseases, Tokyo 162-8640, Japan
[d] National Institute of Health Sciences, Tokyo 158-8501, Japan

ARTICLE INFO

Article history:
Received 14 August 2008
Returned to author for revision
3 September 2008
Accepted 6 October 2008
Available online 14 November 2008

Keywords:
Hepatitis C virus
Core protein
Vimentin

ABSTRACT

Hepatitis C virus (HCV) core protein is essential for virus particle formation. Using HCV core-expressing and non-expressing Huh7 cell lines, Uc39-6 and Uc321, respectively, we performed comparative proteomic studies of proteins in the 0.5% Triton X-100-insoluble fractions of cells, and found that core-expressing Uc39-6 cells had much lower vimentin content than Uc321 cells. In experiments using vimentin-overexpressing and vimentin-knocked-down cells, we demonstrated that core protein levels were affected by cellular vimentin content. When vimentin expression was knocked-down, there was no difference in mRNA level of core protein; but proteasome-dependent degradation of the core protein was strongly reduced. These findings suggest that the turnover rate of core protein is regulated by cellular vimentin content. HCV production was also affected by cellular vimentin content. Our findings together suggest that modulation of hepatic vimentin expression might enable the control of HCV production.

Introduction

Hepatitis C virus (HCV) is a major causative agent of chronic hepatitis (Choo et al., 1989; Kuo et al., 1989). Persistent HCV infection, which develops in at least 70% of infected patients, is strongly correlated with the development of severe liver diseases such as fibrosis, steatosis, cirrhosis, and hepatocellular carcinomas (HCC). Since more than 170 million people in the world are currently infected with HCV (Choo et al., 1989) and there is no treatment completely effective in curing HCV, HCV infection is one of the most important global public health issues. Understanding of the life cycle of HCV and the mechanism by which HCV induces serious liver diseases is crucial for the development of novel anti-HCV strategies.

HCV is an RNA virus of the *Flaviviridae* family and possesses a single-stranded, positive-sense RNA genome of ~9.6 kb (Bartenschlager and Lohmann, 2000). The HCV RNA genome encodes a polyprotein of ~3000 amino acids that is processed by host and viral proteases into 10 individual components including 4 structural and 6 nonstructural proteins (reviewed by Reed and Rice, 2000). HCV core protein is crucial for virus particle production as the structural component of the viral nucleocapsid and as a unit required for formation of the active HCV replication/assembly complex in host cells (Boulant et al., 2007; Miyanari et al., 2007). In addition, the core protein plays pivotal roles in the pathogenesis of HCV infection, as suggested by the finding that transgenic mice expressing core protein in the liver tend to develop liver steatosis with subsequent HCC (Moriya et al., 1998; Moriya et al., 1997). A large number of studies have revealed that a variety of host proteins interact with the core protein (Suzuki et al., 2007). Although these interactions can markedly affect various biological functions in host cells, it is not clearly known yet which interactions and molecules play roles in HCV production or its pathogenicity. Recent exhaustive gene-silencing analyses of host factors using RNAi demonstrated that RNA helicase DDX3, one of the proteins that interacts with the core, is required for HCV RNA replication as well as HCV production (Ariumi et al., 2007; Randall et al., 2007).

In host hepatic cells, HCV core protein is distributed preferentially in the detergent-resistant fractions (Matto et al., 2004), and HCV RNA replication also occurs on detergent-resistant membranes (Aizaki et al., 2004; Shi et al., 2003), suggesting that host factors in the detergent-resistant fractions play roles in core protein functions. In this study, we focused on HCV core protein and the detergent-insoluble proteins of host cells, and performed comparative targeted proteomic analysis of the detergent-insoluble proteins in HCV core-expressing and non-expressing hepatic cells. We identified vimentin as a protein the amount of which was reduced in core-expressing cell lines, and demonstrated that cellular vimentin content affects levels of HCV core protein through the proteasome-mediated protein

* Corresponding author. Fax: +81 3 5285 1157.
E-mail address: fuka@nih.go.jp (M. Fukasawa).
[1] Present address: National Institute of Neuroscience, National Center of Neurology and Psychiatry, Tokyo 187-8502, Japan.

0042-6822/$ – see front matter © 2008 Published by Elsevier Inc.
doi:10.1016/j.virol.2008.10.009

degradation system. Since cellular vimentin levels ultimately affected HCV production, vimentin may be a novel target for strategies of anti-HCV treatment.

Results

Proteomic analysis of detergent-insoluble fractions (DISFs) by second-dimensional polyacrylamide gel electrophoresis (2D-PAGE)/MALDI-QIT-TOF MS

DISFs and detergent-soluble fractions (DSFs) were prepared from HCV core-expressing Uc39-6 and non-expressing Uc321 cells by a sucrose density gradient ultracentrifugation method as described in Materials and methods. Proteins in the DISFs and DSFs were analyzed by immunoblotting with antibodies to HCV core protein and various organelle markers (Fig. 1A). A significant amount of HCV core protein (~70%) was distributed in the DISF of Uc39-6 cells. Nuclear proteins such as laminA/C and laminB were concentrated only in the DISFs of both types of cells, whereas other organelle proteins such as annexin II (plasma membrane), fatty acid synthase (cytosol), prohibitin (mitochondria), and calnexin (endoplasmic reticulum) were detected in the DSFs but not DISFs (Fig. 1A), suggesting that the DISFs in both types of cells contain minor (~15%) discrete populations of cellular proteins. Next, we performed 2D-PAGE analysis of the DISFs in Uc321 and Uc39-6 cells. Proteins in the DISFs were separated by isoelectric focusing (IEF) (pH 4–7) and 12% sodium dodecyl sulfate (SDS)-PAGE, and visualized by SYPRO-Ruby staining (Fig. 1B). Intensity of each spot in 2-D images was compared between Uc321 and Uc39-6 cells. The most difference in DISF proteins between Uc321 and Uc39-6 cells (the Uc39-6/Uc321 ratios of intensity normalized with actin: 10.8–28.0) was detected in the spots numbered as 1 in Fig. 1B (MW ~ 57 kDa, pI ~ 4.7), in which vimentin alone was identified by mass spectrometric analysis. We therefore focused on the relationship between cellular vimentin and core protein in further investigations.

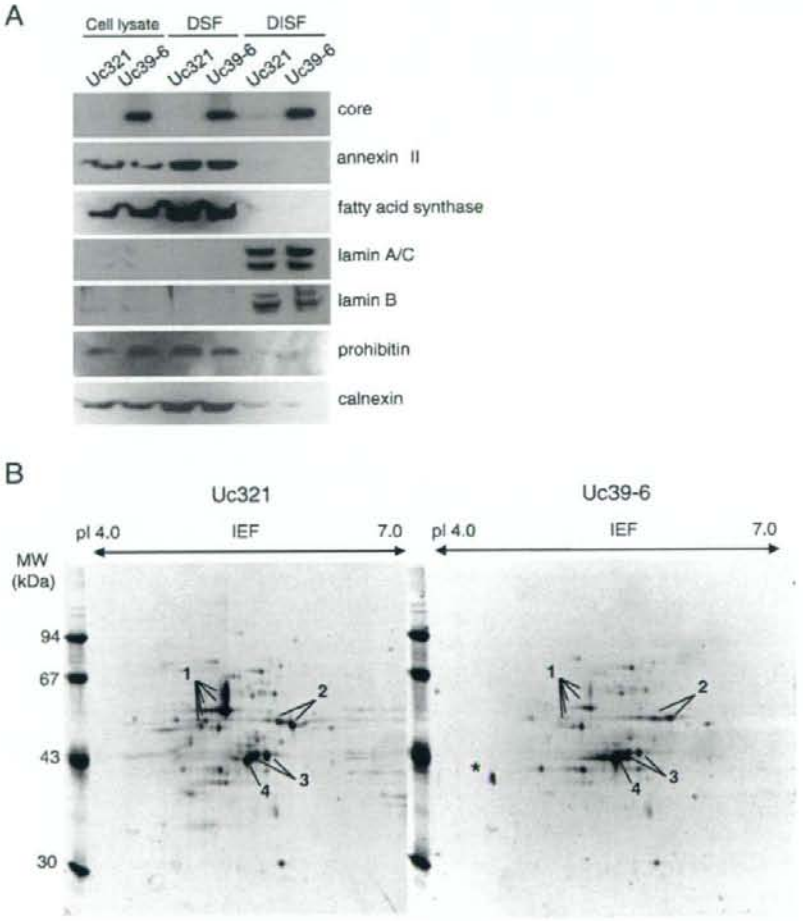

Fig. 1. Immunoblot and 2D-PAGE analysis of DISFs. (A) Total cell lysate fractions (5 μg of protein), DSFs (50 μg of protein), and DISFs (5 μg of protein) from core-expressing Uc39-6 and non-expressing Uc321 cells were analyzed by immunoblotting with antibodies to HCV core protein and various organelle markers as indicated. (B) 2D-PAGE analysis of proteins in DISFs of Uc321 and Uc39-6 cells. Proteins (150 μg) were separated by IEF (pH 4–7), followed by SDS-PAGE on a 12% gel. The gels were stained with SYPRO-Ruby. Major spots, identified as cytoskeletal proteins, are marked: 1, vimentin; 2, cytokeratin 8; 3, cytokeratin 18; 4, actin. *: a non-specific spot.

HCV core-expressing cell lines exhibited reduced vimentin content

To confirm the reduction of vimentin levels in DISFs of HCV core-expressing Uc39-6 cells, immunoblot analysis was performed using anti-vimentin antibody. Uc39-6 cells exhibited lower vimentin contents not only in DISF but also the total cell lysate fraction compared with control Uc321 cells (Fig. 2A). Similar results were obtained in the cell lysate fraction of another independent clone of an HCV core-expressing Huh7 cell line, Uc39-2 (Fig. 2B). Furthermore, a core-expressing hepatic HepG2 cell line, Hep39, also had lower vimentin content than a control cell line, Hepswx (Fig. 2C). These findings exclude the possibility that the reduction of vimentin levels in core-expressing cell lines is a clone- or cell-specific event. Consistent with these findings, levels of vimentin mRNA in Uc39-2 and Uc39-6 cells were also lower than that in Uc321 cells (data not shown). Taken together, these findings demonstrate marked reduction of vimentin expression in HCV core-expressing cell lines.

Cellular vimentin content affects the protein level of HCV core protein

To investigate the relationship between HCV core protein and vimentin, we examined the effect of cellular vimentin content on level of HCV core protein. When the expression of vimentin or control hypoxanthine guanine phosphoribosyltransferase 1 (HPRT) was knocked down in Uc39-6 cells by siRNA treatment, the protein level of HCV core protein in vimentin-knocked-down cells was significantly higher than those in siRNA-untreated and HPRT-knocked-down cells (Fig. 3A). On the other hand, cellular mRNA levels of HCV core protein, corrected for β-actin mRNA content, did not differ substantially among these types of cells (Table 1). These findings revealed that post-translational steps were involved in the increase of HCV core protein level in vimentin-knocked-down cells. Next, we established a vimentin-overexpressing Huh7 cell line, Huh7/vimentin, and compared the level of the core protein in Huh7/vimentin cells with that in control Huh7/hygro cells after transient expression of the core protein with pcEF39neo vector. After 9-day culture with G418 selection, the viabilities of the two types of cells were similar, though the level of expression of the core protein in Huh7/vimentin was significantly lower than that in Huh7/hygro cells (Fig. 3B). These findings demonstrated that level of HCV core protein was inversely correlated with cellular vimentin content, and thus strongly suggested that it was affected by cellular vimentin content.

We further attempted to verify these effects of vimentin using the vimentin-null cell line 1HF5 and the vimentin-expressing control cell line 2CB5, derived from human adrenal carcinoma SW13 cells (Sarria et al., 1990). When 1HF5 and 2CB5 cells were transfected with the core expression vector pcEF39neo and cultured with G418 selection, the viabilities of the two types of cells were similar, though the level of expression of the core protein in 1HF5 cells was much higher than that in 2CB5 cells (Fig. 3C), consistent with the results in Figs. 3A, B. An exogenously vimentin-expressing 1HF5 cell line carrying pcDNA3.1/Hygro/vimentin, 1HF5/vimentin, and a control vimentin-null cell line carrying pcDNA3.1/Hygro, 1HF5/hygro, were then established, and transfected with the green fluorescent protein (GFP)-expressing pcDNA3.1/EGFP vector, the core-coding pcEF39neo vector, or the control pcFE321swxneo vector. After selection under G418 for 9 days, the viabilities of these transfected cells were nearly the same. The levels of expression of GFP were similar in 1HF5/hygro and 1HF5/vimentin cells, while the core protein level in 1HF5/vimentin cells was significantly lower than that in 1HF5/hygro cells (Fig. 3D), consistent with the results in Fig. 3B.

These findings together indicate that cellular vimentin content regulates the level of HCV core protein in post-translational fashion.

Vimentin is involved in proteasomal degradation of core proteins in cells

HCV core proteins are known to be preferentially degraded by the proteasome-dependent pathway (Suzuki et al., 2001). To determine whether cellular vimentin content affects proteasome-dependent degradation of the core protein, we examined the effects of the proteasome inhibitor MG132 on core protein levels in vimentin-knocked-down cells. After Huh7 cells transfected with pCAG/Flag-core (Huh7/Flag-core cells) had been treated with MG132 for 16 h, cellular accumulation of core protein was analyzed by immunoblot (Fig. 4; lanes 3 vs 4), which indicated substantial proteasomal degradation of the core proteins in cultured cells, as described previously (Hope and McLauchlan, 2000; McLauchlan et al., 2002; Suzuki et al., 2001). Huh7/Flag-core cells transfected with control and HPRT siRNA duplexes exhibited similar increases in core protein levels by treatment with MG132 (Fig. 4; lanes 5 vs 6, and 9 vs 10). On the other hand, vimentin-knocked-down Huh7/Flag-core cells that were transfected with vimentin siRNA duplexes exhibited higher content of core protein (lane 7) than the other siRNA-treated cells (lanes 5 and 9), and MG132 treatment resulted in no significant difference in core protein levels in vimentin-knocked-down cells (lanes 7 and 8), indicating that proteasomal degradation of core proteins was markedly inhibited in the vimentin-knocked-down cells. These observations strongly suggested that vimentin plays an important role in the proteasome-mediated proteolytic pathway of the HCV core protein.

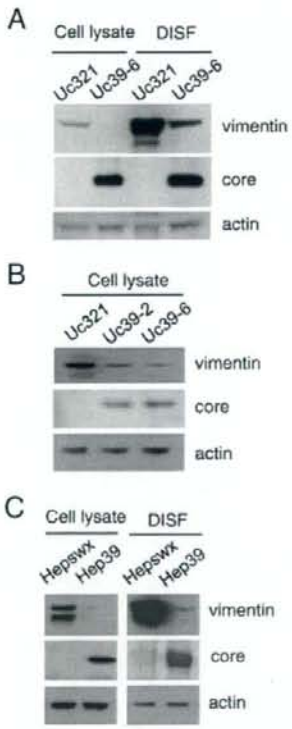

Fig. 2. Immunoblot analysis of vimentin in HCV core-expressing cell lines. Cell lysate fractions and DISFs from various cell lines were analyzed by immunoblotting with antibodies to vimentin, HCV core protein, and β-actin as indicated: cell lysate fractions and DISFs from Uc321 and Uc39-6 cells in (A), cell lysate fractions from Uc321, Uc39-2, and Uc39-6 cells in (B), and cell lysate fractions and DISFs from Hepswx and Hep39 cells in (C). Amounts of protein loaded were 18 μg in (A) and (B), and 5 μg in (C).

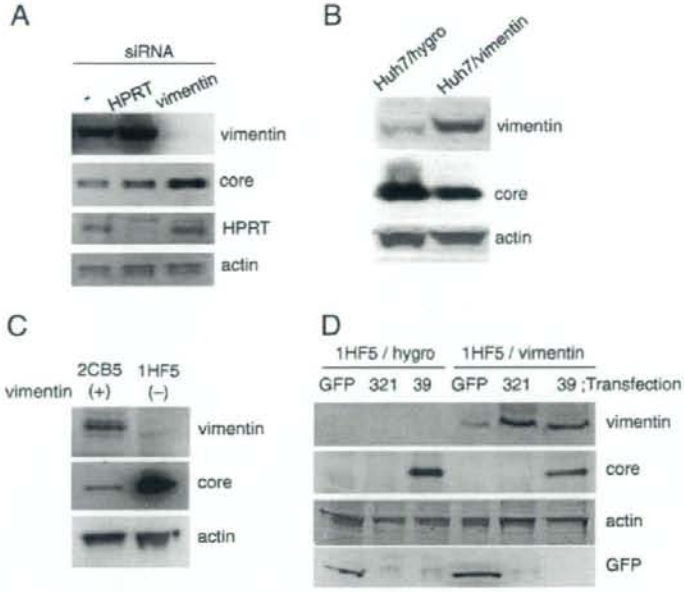

Fig. 3. Effects of cellular vimentin content on the level of expression of HCV core protein. Cellular level of expression of vimentin, HCV core protein, HPRT, β-actin, and GFP were analyzed by immunoblotting of total cell lysates (40 μg of protein) from various cells using specific antibodies. (A) Uc39-6 cells were transfected twice with a 2-day interval without (-) or with vimentin or control HPRT siRNA duplexes. Four days after the first transfection, cell lysates were collected and analyzed. (B) Huh7/hygro and Huh7/vimentin cells were transfected with the core protein-expression vector pcEF39neo, and selected under 1 mg/ml of G418 for 9 days. (C) The 2CB5 (vimentin+) and 1HF5 (vimentin−) lines of SW13 cells were transfected with pcEF39neo, and selected under 1 mg/ml of G418 for a week, followed by additional 2-week culture in normal culture medium. (D) 1HF5/hygro and 1HF5/vimentin cells were transfected with pcDNA3.1/EGFP (GFP), pcFE321swxneo (321), or pcEF39neo (39), and selected under 1 mg/ml of G418 for 9 days.

Under the various siRNA-treated conditions in Fig. 4, we also examined the protein levels of p53, one of the endogeneous host proteins the degradation of which is mainly regulated by proteasomal system (Morimoto et al., 2008). The pattern of p53 protein levels was very similar to that of core protein levels (Fig. 4), suggesting that the vimentin-dependent proteasomal degradation is not specific for the viral core protein. Vimentin-dependent proteasomal degradation system might be generally important for the turnover of endogeneous cellular proteins as well as the viral core protein.

Cellular vimentin contents affect HCV production

Since the level of expression of HCV core protein was affected by cellular vimentin content, we examined whether HCV production was also affected by cellular vimentin content. Infectious HCV (JFH1 strain) particles were used for the following infection assays. HCV production activity was determined by quantification of HCV core protein levels in the infected cells and culture supernatants. We first tested the effect of vimentin knockdown on HCV production. Examination of HCV-infected Huh7 cells treated with vimentin siRNA revealed higher amounts of HCV core protein in both cells and culture medium than examination of non-treated and control HPRT siRNA-treated cells (Fig. 5A). To examine whether the core protein levels in the cell-cultured media reflect the content of infectious HCV particles in them, Huh7 cells were treated with cell-cultured medium containing equal amounts (1.4 fmol) of the core protein collected from each type of cell described in Fig. 5A, and cellular levels of production of the core protein were determined by immunoblot analysis. They were nearly the same among the cells treated with each culture medium (Fig. 5B). These findings indicated that reduction of vimentin expression in Huh7 cells leads to more active HCV production and enhanced release to the supernatant.

We next examined the effects of vimentin overexpression on HCV production. When vimentin-overexpressing Huh7/vimentin and control Huh7/hygro cells were infected with HCV particles, Huh7/vimentin cells exhibited lower amounts of intracellular and extracellular HCV core protein than Huh7/hygro cells (Fig. 5C). Consistent with the results in Fig. 5A, these findings suggested that higher expression of vimentin in host cells resulted in lower HCV production.

We also examined the effect of vimentin knockdown on HCV RNA replication using a JFH1-subgenomic replicon (Fig. 5D). There were no significant differences in replication activities between vimentin-knocked-down cells and the other control cells. These findings indicated that cellular level of vimentin has no effects on HCV non-structural proteins which serve as a unit of RNA replication machinery of HCV. Collectively, these results demonstrated that HCV production activity but not HCV-RNA replication was inversely correlated with cellular vimentin content.

Table 1
mRNA levels of HCV core protein and β-actin in vimentin-knocked-down Uc39-6 cells

	siRNA		
	-	HPRT	vimentin
HCV core ($\times 10^4$ copies/μg total RNA)	2.9±0.3	1.7±0.1	3.0±0.2
β-actin ($\times 10^7$ copies/μg total RNA)	3.0±0.1	1.4±0.1	2.3±0.0
HCV core/β-actin[a]	1	1.3	1.3

Total RNA was isolated from Uc39-6 cells that had been treated twice with a 2-day interval with HPRT siRNA duplexes, with vimentin siRNA duplexes or without (-) either of them, and cultured for 4 days. mRNA levels of HCV core protein and β-actin (a control housekeeping gene) were determined by quantitative real-time PCR. Values are the mean ± SD for three determinations.

[a] Numbers represent the relative amounts of HCV core protein mRNA normalized to β-actin level.

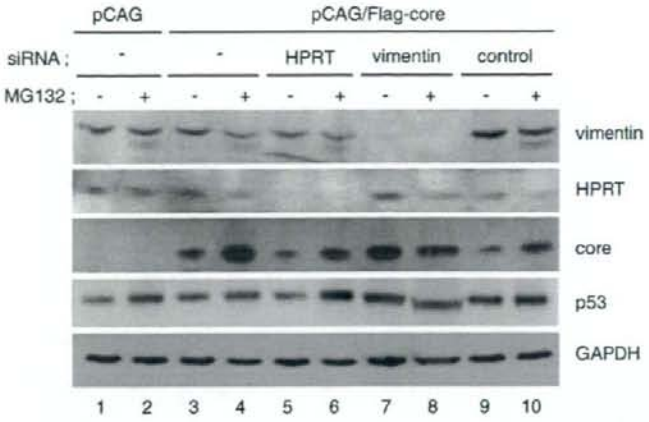

Fig. 4. Effects of the proteasome inhibitor MG132 on level of expression of HCV core protein in Huh7 cells. siRNA duplexes of control, HPRT, or vimentin, together with the core protein-expression vector pCAG/Flag-core, were transfected into Huh7 cells. After 2 days, transfection of these siRNAs was repeated. Cells were further cultured for 2 days and treated with (+) or without (−) MG132 (50 μM) for 16 h. Equivalent amounts of cell lysates were analyzed by immunoblotting with antibodies to vimentin, HPRT, core protein, p53, and GAPDH.

Furthermore, expression of vimentin and HCV core protein in Huh7 cells after HCV infection was observed by immunofluorescence microscopy (Fig. 5E), and the fluorescent intensity of vimentin in core-positive and core-negative Huh7 cells under HCV-infected conditions was determined (Fig. 5F). HCV-infected cells stained with the core-specific antibody always had lower vimentin content (Figs. 5E, F). Moreover, as shown in Fig. 5F, HCV core-negative cells exhibited more variable vimentin levels, whereas the core-positive cells had vimentin levels within a narrow range. These observations, which showed that a Huh7 cell population with lower vimentin content can preferentially produce HCV, were consistent with the results shown in Figs. 5A, C.

Finally, we examined the effects of MG132 on HCV core protein levels in HCV-infected cells in which vimentin was knocked-down or overexpressed. In the presence of MG132, non-treated and control HPRT siRNA-treated cells showed the significant increase of cellular HCV core protein levels, whereas vimentin-knocked-down cells did not (Fig. 5G). These results were consistent with those using HCV core-expressing cells (Fig. 4). HCV core content in vimentin-overexpressing Huh7/vimentin cells was lower than that in control Huh7/hygro cells, but after MG132 treatment Huh7/vimentin and Huh7/hygro cells showed the similar HCV core protein levels (Fig. 5H). Taken together, these results demonstrated the significant involvement of vimentin in proteasome-dependent degradation of HCV core protein in HCV-infected cells (Figs. 5G, H), as well as in HCV core-expressing cells (Fig. 4).

Discussion

By comparative proteomic analysis of the detergent-insoluble proteins in HCV core-expressing and non-expressing Huh7 cell lines, vimentin, an intermediate filament protein, was identified as the protein with the most dramatic reduction in level in the detergent-insoluble fraction of HCV core-expressing Uc39-6 cells (Figs. 1B and 2). On the other hand, there were no significant differences in the amounts of other major proteins including cytoskeletal components such as actin and cytokeratin 8/18 in the detergent-insoluble fractions between the core-expressing and non-expressing cells (Fig. 1B). These findings, together with similar results for other core-expressing cells (Fig. 2), suggested the existence of a specific relationship between the core protein and cellular vimentin. Consistent with these findings, immunofluorescence microscopic analysis of core-expressing cells (data not shown) and HCV-infected cells (Figs. 5E, F) showed that cells with intrinsic lower amount of vimentin are more permissive for higher HCV core protein content.

Knockdown of vimentin expression by siRNA treatment resulted in an increase in HCV core protein levels (Fig. 3A), while overexpression of vimentin reduced core protein contents (Fig. 3B). Similar results were obtained in the experiments using the vimentin-null cell line 1HF5 derived from SW13 cells (Figs. 3C and D). On the other hand, transient knockdown and overexpression of the core proteins in Uc39-6 and Huh7 cells, respectively, did not result in differences in cellular vimentin content (data not shown). These findings indicated that cellular vimentin level affects the level of expression of the core protein but not vice versa. Although transient expression of the core protein did not affect cellular vimentin content, why do various stable cell lines expressing the core protein have lower vimentin level? Since it was very hard to establish the cells stably expressing the core protein, we speculate that only the minor cell population innately having lower vimentin content was able to maintain the substantial core expression levels and was therefore selected.

We next demonstrated that vimentin affects core protein levels in post-translational fashion (Table 1) and is required for the proteasomal degradation of core protein in core-expressing cells (Fig. 4) and also in HCV-infected cells (Figs. 5G, H). Many studies with proteasome inhibitors have shown that a major pathway of degradation of core protein is mediated by the proteasomal system (Hope and McLauchlan, 2000; McLauchlan et al., 2002; Moriishi et al., 2003; Suzuki et al., 2001). PA28γ, a REG family proteasome activator also known as REGγ and Ki antigen, which is located in the nucleus, was shown to play an important role in the proteasomal degradation of the core protein (Moriishi et al., 2003). It was recently reported that the ubiquitin ligase E6AP, which is distributed in the perinuclear cytoplasm and colocalized with the core protein, is also involved in ubiquitylation and degradation of core protein (Shirakura et al., 2007). Vimentin filaments extend from the nuclear membrane toward the cell periphery. In addition, vimentin is known to colocalize with ubiquitinated protein aggregates and form aggresomes when the capacity of the proteasome is exceeded (Johnston et al., 1998). Pull-down assays against the core protein in core-expressing Huh7 cells indicated that a minor portion of cellular vimentin can interact with HCV core protein (data not shown), as

Kang et al. had reported previously (Kang et al., 2005). Co-staining of cellular vimentin and the core protein on immunofluorescence microscopy also supported the existence of a minor but definite association between them (data not shown). Based on these findings, we speculate that vimentin plays a role in the transport of the core protein to the nucleus, where it is then degraded, although further biochemical studies will be needed to demonstrate this.

HCV core protein is distributed mainly in the ER and lipid droplets in host cells (Barba et al., 1997), and the ER membrane associating the lipid droplets with core protein has been recognized as a site important for HCV production, particularly HCV RNA replication and virus particle assembly (Boulant et al., 2007; Miyanari et al., 2007). Vimentin is also closely associated with lipid droplets (Brasaemle et al., 2004; Lieber and Evans, 1996; Schweitzer and Evans, 1998). Thus, in addition to its degradative modulation of core protein, vimentin might also affect the function of lipid droplets and consequently inhibit HCV production. The effects of vimentin knock-down and overexpression on HCV production were actually stronger at the extracellular core protein level (secretion

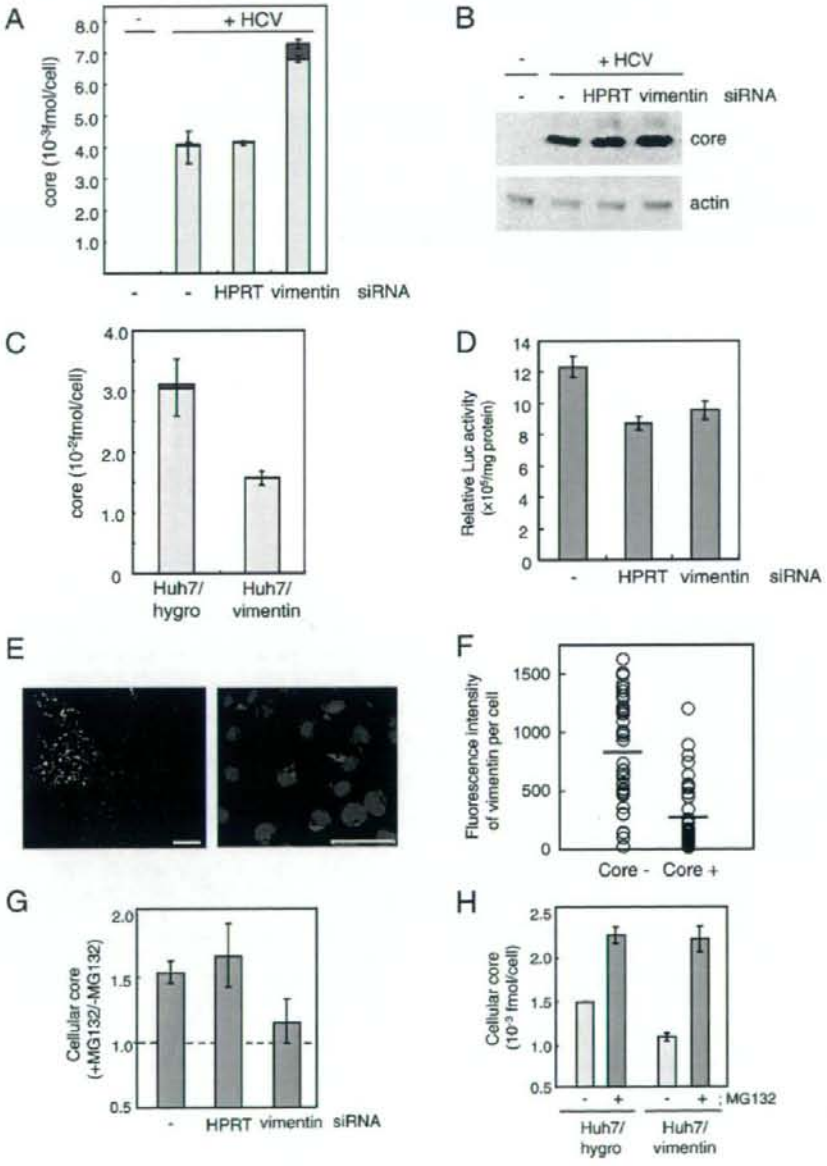

of the virus) than at the intracellular core protein level (Figs. 5A, C), suggesting additional activity of vimentin in the processes of HCV particle release.

Since the level of expression of vimentin in carcinomas is correlated with parameters of malignant potential such as tumor grade and tumor invasion, vimentin has been used as a marker of malignant tumors (Bannasch et al., 1982). It has indeed been reported that some HCV-infected patients with hepatocellular carcinoma exhibited up-regulation of vimentin expression in tumor tissue (Kim et al., 2003) although further statistical studies are required to clearly demonstrate this. Tanaka et al. noted that in livers of HCV-infected patients with hepatocelllular carcinoma the virus existed predominantly in non-cancerous tissue, at levels 10- to 100-fold higher than in cancerous tissue (Tanaka et al., 2004). These observations in human liver samples suggest that the reduction in HCV levels in hepatic tumor can be explained by the increase of vimentin expression in tumor, consistent with our findings for cultured cells.

In this study we demonstrated that cellular vimentin expression enhanced the proteasomal degradation of core protein and eventually restricted HCV production. Vimentin itself and sites of vimentin/core interaction may thus be novel targets of treatment using anti-HCV strategies.

Materials and methods

Antibodies

Mouse monoclonal antibodies to annexin II, fatty acid synthase, calnexin, lamin A/C, and GFP were purchased from BD Transduction Laboratories. Mouse monoclonal antibodies to HCV core protein, prohibitin, and glyceraldehyde-3-phosphate dehydrogenase (GAPDH) were from Anogen, Lab Vision, and Abcam, respectively. Rabbit polyclonal antibodies to vimentin, lamin B1, p53, and HPRT were from Santa Cruz Biotechnology Inc., while those to actin were from Biomedical Technologies Inc.

Plasmids

The mammalian expression vector of HCV core protein, pcEF39neo (Ruggieri et al., 1997), and the empty vector pcEF321swxneo (Harada et al., 1995) were described previously. The mammalian expression vector of Flag-tagged HCV core protein, pCAG/Flag-core, and the empty vector, pCAG, were described previously (Moriishi et al., 2003). For construction of a mammalian expression vector of vimentin, pcDNA3.1/Hygro/vimentin, vimentin fragment was amplified by PCR using the reverse-transcribed cDNAs of Huh7 cells as a template. The PCR primer pairs used were 5′-GCCATGTCCACCAGGTCCGTGTCC-3′ and 5′-TTATTATTCAAGGTCATCGTGATG-3′. The PCR products were inserted into the EcoRV site of pBluescript SKII(+). pBluescript SK(+)/vimentin was digested with Hind III and Xba I, and the vimentin fragment was inserted into pcDNA3.1/Hygro (Invitrogen), which had been digested with Hind III and Xba I. For construction of pcDNA3.1/EGFP, EGFP fragment was prepared by digestion of pEGFP-N1 (Clontech Laboratories, Inc.) with Nhe I and Hind III and inserted into pcDNA3.1/Hygro, which had been digested with Nhe I and Hind III. The subgenomic replicon constructs, pSGR-JFH1/Luc (wild type) and pSGR-JFH1/Luc-GND (GND mutation in the NS5B sequence), with the firefly luciferase reporter gene were described previously (Kato et al., 2005).

Cell lines

All hepatic cells used in this study were plated on collagen-coated dishes (Asahi Techno Glass, Japan). Human hepatic Huh7 and Huh7.5.1 cells were grown in normal culture medium [Dulbecco's modified Eagle's medium (DMEM) (KOJIN BIO, Japan) supplemented with 10% fetal bovine serum (FBS), 100 U/ml Penicillin G, and 100 mg/ml streptomycin sulfate] containing 0.1 mM non-essential amino acids (GIBCO) under a 5% CO_2 atmosphere at 37 °C. We used human hepatic cell lines constitutively expressing HCV core protein, including Hep39 from HepG2 cells (Harada et al., 1995; Ruggieri et al., 1997) and Uc39-2 and Uc39-6 from Huh7 cells (Fukasawa et al., 2006; Sato et al., 2006). Huh7 and HepG2 cell lines carrying the empty vector, Hepswx and Uc321, respectively, were used as a mock control. All of these stable transfectants were maintained in normal culture medium containing 1 mg/ml G418 (Sigma). The human adrenal carcinoma cell line SW13, the subtypes 2CB5 and 1HF5 of which do or do not express vimentin, respectively (Sarria et al., 1990), was maintained in normal culture medium. When the pcDNA3.1/EGFP vector was transfected into 2CB5 and 1HF5 cells, the percentage of GFP-positive cells was 56.3% and 53.6%, respectively, 2 days after transfection ($n=3$), indicating that there was no difference in the transfection efficiency between these cells. To establish vimentin-overexpressing cells, pcDNA3.1/Hygro/vimentin was transfected into 1HF5 and Huh7 cells using FuGENE 6 transfection regent (Roche). The vimentin-overexpressing Huh7 and 1HF5 cells were selected under hygromycin for 2 weeks and cloned to obtain Huh7/vimentin cells and 1HF5/vimentin cells, respectively. Huh7 and 1HF5 cells carrying the empty vector pcDNA/Hygro were also established, as Huh7/hygro cells and 1HF5/hygro cells, respectively.

Preparation of DISFs

Confluent monolayers of Uc321 and Uc39 cells in four culture dishes (150 mm inner diameter) were harvested by trypsinization, and 1.5×10^7 cells of each were pelleted by centrifugation (218 ×g for 5 min at 4 °C). After washing with PBS three times, each cell pellet was resuspended in 1 ml of lysis buffer [10 mM HEPES-HCl, pH 7.5, 10 mM NaCl, 140 mM KCl, 0.5 mM DTT, 0.5% Triton X-100 (Pierce Biotechnology), 10 mM NaF, Complete™ EDTA-free (Roche)] (i.e. a 20% cell suspension). The cell suspension was lysed with a ball-bearing homogenizer (Hope et al., 2002). The soluble fraction (designated the detergent-soluble fraction, DSF) containing ~85% of the total cellular proteins was collected by centrifugation of the cell

Fig. 5. HCV production in vimentin-knockdown and vimentin-overexpressing Huh7 cells. (A) Huh7 cells (5×10^4 cells) in 48-well plates were incubated with or without HCV particles (including 8.0 fmol of core protein) for 6 h, and then treated twice with a 3-day interval without (−) or with siRNA duplexes of HPRT or vimentin. After 7-day culture, the amounts of HCV core protein per cell in cells (light gray bar) and culture medium (dark gray bar) were determined. $n=3$. (B) Culture medium was collected at day 6 in the infection experiment described above in (A). The concentration of HCV core protein in these samples of medium was adjusted to 2.7 fmol/ml with fresh medium. Cells were infected with these samples of medium containing 1.4 fmol of HCV core protein for 2 days, and harvested after 7-day incubation. Infectivity was analyzed by the immunoblotting of cell lysates with antibodies to HCV core protein and β-actin. (C) Vimentin-overexpressing Huh7/vimentin and control Huh7/hygro cells infected with HCV were harvested after 7-day incubation. The amounts of HCV core protein per cell in cells (light gray bar) and culture medium (dark gray bar) were determined. (D) Huh7 cells harboring the HCV subgenomic replicon containing a luciferase reporter gene were transfected without (−) or with siRNA duplexes of HPRT or vimentin. After 2.5-day culture, luciferase activity in cell extracts was determined. $n=3$. (E) Immunofluorescence microscopic analysis of HCV-infected Huh7 cells. After infection with HCV, Huh7 cells were cultured for 6 days. HCV core protein (green) and vimentin (red) were then detected with specific antibodies. Nuclei (blue) were stained with DAPI. Two views showing low and high magnifications are displayed. Bars, 100 μm in the left panel; 50 μm in the right panel. (F) Under the HCV-infected conditions in panel E, fluorescence intensity of vimentin in core-positive and core-negative Huh7 cells was determined by line profile analysis. $n=40$. Statistical significance of differences in fluorescence intensity of vimentin between core-positive and core-negative cells was evaluated using Student's t test, showing $p<10^{-8}$. (G) As in (A), Huh7 cells were incubated with HCV particles, and then treated twice with a 2-day interval without (−) or with siRNA duplexes of HPRT or vimentin. After 4.5-day culture, cells were treated with (+) or without (−) MG132 (50 μM) for 16 h. In each culture condition, the ratio of HCV core protein level in the MG132-treated cells to that in MG132-untreated cells was determined. $n=3$. (H) Huh7/vimentin and Huh7/hygro cells infected with HCV were cultured for 4 days and treated with (+) or without (−) MG132 (50 μM) for 16 h. The amounts of cellular core protein per cell were determined. $n=3$.

lysate performed twice at 218 ×g for 5 min at 4 °C. The insoluble pellet was suspended in 2 ml of lysis buffer containing 1.62 M sucrose and then centrifuged at 10,000 ×g for 1 h at 4 °C. The pellet was resuspended in 1 ml of lysis buffer containing 1.0 M sucrose and layered over 2 ml of lysis buffer containing 2.0 M sucrose. After centrifugation at 50,000 ×g for 2 h at 4 °C, the precipitated fraction containing ~15% of total cellular proteins was collected and resuspended in lysis buffer containing 0.25 M sucrose at a concentration of 3 mg protein/ml (designated the detergent-insoluble fraction, DISF). Each fraction was stored at −80 °C until use. The protein concentrations in these preparations were determined with BCA protein assay reagents (Pierce Biotechnology) using BSA as a standard.

2D-PAGE/MALDI-QIT-TOF MS analysis

The DISF (0.15 mg protein) of each cell line was cleaned using a PlusOne™ 2-D Clean Up kit (GE Healthcare) and resuspended in rehydration solution containing 9 M urea, 4% CHAPS, 65 mM dithioerythritol, and 0.5% ampholyte. The first-dimensional IEF was performed with an Immobiline Dry Strip pH 4–7 according to the manufacturer's instruction (GE Healthcare). The second-dimensional electrophoresis was carried out on 12% SDS-polyacrylamide gel, and the gel was stained with SYPRO-Ruby (Bio-Rad). Spot detection and comparison in 2D images were accomplished with PDQuest™ 2-D analysis software ver. 7.3 (Bio-Rad). The protein bands were excised from the gel and subjected to in-gel trypsin digestion. The tryptic peptide mixtures were analyzed by MALDI-QIT-TOF MS (AXIMA-QIT, Shimazu Biotech, Japan) as described previously (Sato et al., 2006; Shevchenko et al., 1996). Mascot software (Matrix Science) was used for protein identification.

Immunoblot analysis

The proteins were separated by electrophoresis in precast NuPAGE 10% or 12% Bis–Tris gels (Invitrogen), and then transferred to a polyvinylidene difluoride membrane. The membranes were blocked overnight at 4 °C or for 60 min at room temperature in Tris-buffered saline containing 0.1% Tween 20 and 5% skim milk. The blots were probed with the first antibodies at 1:1000 dilution for 60 min at room temperature and then incubated with horseradish peroxidase (HRP)-conjugated goat anti-rabbit IgG (Bio-Rad) or HRP-conjugated goat anti-mouse IgG (GE Healthcare) at 1:2000 dilution for 45 min. Detection of immunoreactive proteins was performed using an ECL system (GE Healthcare).

Quantitative real-time PCR analysis

Cellular total RNAs were prepared with an RNeasy kit (Qiagen). The total RNA fraction (1 μg) was processed directly to cDNA using a Transcriptor First Strand cDNA Synthesis Kit (Roche). Of the total 20 μl cDNA solution, an aliquot of 0.5–2 μl was used for each real-time PCR assay. The PCR primers used for HCV core protein were: forward, 5′-AGGAAGACTTCCGAGCG-3′, and reverse, 5′-GGGTGACAGGAGCCATC-3′. The PCR primers for actin were obtained from the LightCycler™-Primer Set (Roche). Quantitative real-time PCR was carried out in a LightCycler (Roche) using LightCycler-FastStart DNA Master SYBR Green I (Roche).

Transfection of siRNA

Subconfluent cells cultured in a 48-well plate were transfected twice at a 2- or 3-day interval with 30 nM of vimentin-specific, HPRT-specific, or negative control (Invitrogen) siRNA duplexes using Lipofectamine RNAiMAX (Invitrogen) following the manufacturer's instructions. The siRNA target sequences were as follows: vimentin (sense), 5′-ACCTTGAACGCAAAGTGGAATCTTT-3′; HPRT-S1 (sense), 5′-AAGCCAGACUUUGUUGGAUUUGAAA-3′.

Infection of Huh7 cells with HCV

Infectious HCV (JFH1 strain) particles were produced in Huh7.5.1 cells as described previously (Wakita et al., 2005). Culture supernatant containing infectious HCV particles was collected and stored at −80 °C until use. Subconfluent naïve Huh7, Huh7/hygro, or Huh7/vimentin cells in 24-well or 48-well plates were exposed to normal culture medium containing HCV particles (1.4–8 fmol core protein/well, corresponding to moi = 0.0175–0.1) for 6 h at 37 °C. Cells were then washed and maintained in 500 μl (24-well) or 250 μl (48-well) of normal culture medium for 6–7 days at 37 °C. To determine HCV production activity, the amounts of HCV core protein in the culture medium and cell lysates were quantified with an enzyme-linked immunosorbent assay (ELISA) (Ortho® HCV antigen ELISA test, Ortho-Clinical Diagnostics, Japan).

Assay for activity of HCV genomic RNA replication

The RNAs (30 μg) transcribed from pSGR-JFH1/Luc and pSGR-JFH1/Luc-GND (Kato et al., 2005) were transfected into Huh7 cells (1.6×10^6 cells) by electroporation. Transfected cells in normal culture medium were immediately seeded into 48-well plates at 9.0×10^4 cells/well. Four hours after transfection, siRNAs were also transfected into these cells. After incubation for 2.5 days, cells were harvested and the luciferase activity in cell lysates was determined with the Luciferase Assay System (Promega). Since the luciferase activities of the JFH1/Luc replicon were ~400-fold higher than those of the JFH1/Luc-GND mutant replicon, background luciferase activity, which is independent of replication activity, was very low in our experimental conditions.

Immunofluorescence microscopy

Cells cultured on glass cover slips (in 24-well plates) were fixed in 1% formaldehyde-PBS for 1 h at 4 °C, permeabilized in PBS containing 0.1% Triton X-100 for 5 min, and washed twice with PBS. The cell monolayers were incubated with rabbit anti-vimentin antibodies (1:100) and mouse anti-HCV core protein antibodies (1:100) for 60 min at room temperature. After washing with PBS, the cells were incubated with Alexa488-conjugated anti-mouse IgG, Alexa594-conjugated anti-rabbit IgG, and DAPI (4′, 6′-diamidino-2-phenylindole) (Invitrogen) for 60 min at 4 °C. Coverslips were washed with PBS and mounted on glass slides. Immunofluorescence was visualized and quantitated with a confocal laser-scanning microscope (Axiovert 100M, Carl Zeiss) equipped with a LSM510 system (Carl Zeiss).

Acknowledgments

Huh-7.5.1 cells and Huh-7 cells were kindly provided by F. V. Chisari (Scripps Research Institute).

This work was supported in part by grants-in-aid from the Ministry of Health, Labor, and Welfare of Japan, and by grants-in-aid from the Ministry of Education, Culture, Sports, Science, and Technology of Japan.

References

Aizaki, H., Lee, K.J., Sung, V.M., Ishiko, H., Lai, M.M., 2004. Characterization of the hepatitis C virus RNA replication complex associated with lipid rafts. Virology 324 (2), 450–461.

Ariumi, Y., Kuroki, M., Abe, K., Dansako, H., Ikeda, M., Wakita, T., Kato, N., 2007. DDX3 DEAD-box RNA helicase is required for hepatitis C virus RNA replication. J. Virol. 81 (24), 13922–13926.

Bannasch, P., Zerban, H., Mayer, D., 1982. The cytoskeleton in tumor cells. Pathol. Res. Pract. 175 (2–3), 196–211.

Barba, G., Harper, F., Harada, T., Kohara, M., Goulinet, S., Matsuura, Y., Eder, G., Schaff, Z., Chapman, M.J., Miyamura, T., Brechot, C., 1997. Hepatitis C virus core protein shows a cytoplasmic localization and associates to cellular lipid storage droplets. Proc. Natl. Acad. Sci. U. S. A. 94 (4), 1200–1205.

Bartenschlager, R., Lohmann, V., 2000. Replication of hepatitis C virus. J. Gen. Virol. 81 (Pt 7), 1631–1648.
Boulant, S., Targett-Adams, P., McLauchlan, J., 2007. Disrupting the association of hepatitis C virus core protein with lipid droplets correlates with a loss in production of infectious virus. J. Gen. Virol. 88 (Pt 8), 2204–2213.
Brasaemle, D.L., Dolios, G., Shapiro, L., Wang, R., 2004. Proteomic analysis of proteins associated with lipid droplets of basal and lipolytically stimulated 3T3-L1 adipocytes. J. Biol. Chem. 279 (45), 46835–46842.
Choo, Q.L., Kuo, G., Weiner, A.J., Overby, L.R., Bradley, D.W., Houghton, M., 1989. Isolation of a cDNA clone derived from a blood-borne non-A, non-B viral hepatitis genome. Science 244 (4902), 359–362.
Fukasawa, M., Tanaka, Y., Sato, S., Ono, Y., Nitahara-Kasahara, Y., Suzuki, T., Miyamura, T., Hanada, K., Nishijima, M., 2006. Enhancement of de novo fatty acid biosynthesis in hepatic cell line Huh7 expressing hepatitis C virus core protein. Biol. Pharm. Bull. 29 (9), 1958–1961.
Harada, T., Kim, D.W., Sagawa, K., Suzuki, T., Takahashi, K., Saito, I., Matsuura, Y., Miyamura, T., 1995. Characterization of an established human hepatoma cell line constitutively expressing non-structural proteins of hepatitis C virus by transfection of viral cDNA. J. Gen. Virol. 76 (Pt 5), 1215–1221.
Hope, R.G., McLauchlan, J., 2000. Sequence motifs required for lipid droplet association and protein stability are unique to the hepatitis C virus core protein. J. Gen. Virol. 81 (Pt 8), 1913–1925.
Hope, R.G., Murphy, D.J., McLauchlan, J., 2002. The domains required to direct core proteins of hepatitis C virus and GB virus-B to lipid droplets share common features with plant oleosin proteins. J. Biol. Chem. 277 (6), 4261–4270.
Johnston, J.A., Ward, C.L., Kopito, R.R., 1998. Aggresomes: a cellular response to misfolded proteins. J. Cell Biol. 143 (7), 1883–1898.
Kang, S.M., Shin, M.J., Kim, J.H., Oh, J.W., 2005. Proteomic profiling of cellular proteins interacting with the hepatitis C virus core protein. Proteomics 5 (8), 2227–2237.
Kato, T., Date, T., Miyamoto, M., Sugiyama, M., Tanaka, Y., Orito, E., Ohno, T., Sugihara, K., Hasegawa, I., Fujiwara, K., Ito, K., Ozasa, A., Mizokami, M., Wakita, T., 2005. Detection of anti-hepatitis C virus effects of interferon and ribavirin by a sensitive replicon system. J. Clin. Microbiol. 43 (11), 5679–5684.
Kim, W., Oe Lim, S., Kim, J.S., Ryu, Y.H., Byeon, J.Y., Kim, H.J., Kim, Y.I., Heo, J.S., Park, Y.M., Jung, G., 2003. Comparison of proteome between hepatitis B virus- and hepatitis C virus-associated hepatocellular carcinoma. Clin. Cancer Res. 9 (15), 5493–5500.
Kuo, G., Choo, Q.L., Alter, H.J., Gitnick, G.L., Redeker, A.G., Purcell, R.H., Miyamura, T., Dienstag, J.L., Alter, M.J., Stevens, C.E., et al., 1989. An assay for circulating antibodies to a major etiologic virus of human non-A, non-B hepatitis. Science 244 (4902), 362–364.
Lieber, J.G., Evans, R.M., 1996. Disruption of the vimentin intermediate filament system during adipose conversion of 3T3-L1 cells inhibits lipid droplet accumulation. J. Cell. Sci. 109 (Pt 13), 3047–3058.
Matto, M., Rice, C.M., Aroeti, B., Glenn, J.S., 2004. Hepatitis C virus core protein associates with detergent-resistant membranes distinct from classical plasma membrane rafts. J. Virol. 78 (21), 12047–12053.
McLauchlan, J., Lemberg, M.K., Hope, G., Martoglio, B., 2002. Intramembrane proteolysis promotes trafficking of hepatitis C virus core protein to lipid droplets. EMBO J. 21 (15), 3980–3988.
Miyanari, Y., Atsuzawa, K., Usuda, N., Watashi, K., Hishiki, T., Zayas, M., Bartenschlager, R., Wakita, T., Hijikata, M., Shimotohno, K., 2007. The lipid droplet is an important organelle for hepatitis C virus production. Nat. Cell Biol. 9 (9), 1089–1097.
Moriishi, K., Okabayashi, T., Nakai, K., Moriya, K., Koike, K., Murata, S., Chiba, T., Tanaka, K., Suzuki, R., Suzuki, T., Miyamura, T., Matsuura, Y., 2003. Proteasome activator PA28gamma-dependent nuclear retention and degradation of hepatitis C virus core protein. J. Virol. 77 (19), 10237–10249.
Morimoto, T., Fujita, M., Kawamura, T., Sunagawa, Y., Takaya, T., Wada, H., Shimatsu, A., Kita, T., Hasegawa, K., 2008. Myocardial regulation of p300 and p53 by doxorubicin involves ubiquitin pathways. Circ. J. 72 (9), 1506–1511.
Moriya, K., Yotsuyanagi, H., Shintani, Y., Fujie, H., Ishibashi, K., Matsuura, Y., Miyamura, T., Koike, K., 1997. Hepatitis C virus core protein induces hepatic steatosis in transgenic mice. J. Gen. Virol. 78 (Pt 7), 1527–1531.
Moriya, K., Fujie, H., Shintani, Y., Yotsuyanagi, H., Tsutsumi, T., Ishibashi, K., Matsuura, Y., Kimura, S., Miyamura, T., Koike, K., 1998. The core protein of hepatitis C virus induces hepatocellular carcinoma in transgenic mice. Nat. Med. 4 (9), 1065–1067.
Randall, G., Panis, M., Cooper, J.D., Tellinghuisen, T.L., Sukhodolets, K.E., Pfeffer, S., Landthaler, M., Landgraf, P., Kan, S., Lindenbach, B.D., Chien, M., Weir, D.B., Russo, J.J., Ju, J., Brownstein, M.J., Sheridan, R., Sander, C., Zavolan, M., Tuschl, T., Rice, C.M., 2007. Cellular cofactors affecting hepatitis C virus infection and replication. Proc. Natl. Acad. Sci. U. S. A. 104 (31), 12884–12889.
Reed, K.E., Rice, C.M., 2000. Overview of hepatitis C virus genome structure, polyprotein processing, and protein properties. Curr. Top. Microbiol. Immunol. 242, 55–84.
Ruggieri, A., Harada, T., Matsuura, Y., Miyamura, T., 1997. Sensitization to Fas-mediated apoptosis by hepatitis C virus core protein. Virology 229 (1), 68–76.
Sarria, A.J., Nordeen, S.K., Evans, R.M., 1990. Regulated expression of vimentin cDNA in cells in the presence and absence of a preexisting vimentin filament network. J. Cell Biol. 111 (2), 553–565.
Sato, S., Fukasawa, M., Yamakawa, Y., Natsume, T., Suzuki, T., Shoji, I., Aizaki, H., Miyamura, T., Nishijima, M., 2006. Proteomic profiling of lipid droplet proteins in hepatoma cell lines expressing hepatitis C virus core protein. J. Biochem. (Tokyo) 139 (5), 921–930.
Schweitzer, S.C., Evans, R.M., 1998. Vimentin and lipid metabolism. Sub-cell. Biochem. 31, 437–462.
Shevchenko, A., Wilm, M., Vorm, O., Jensen, O.N., Podtelejnikov, A.V., Neubauer, G., Shevchenko, A., Mortensen, P., Mann, M., 1996. A strategy for identifying gel-separated proteins in sequence databases by MS alone. Biochem. Soc. Trans. 24 (3), 893–896.
Shi, S.T., Lee, K.J., Aizaki, H., Hwang, S.B., Lai, M.M., 2003. Hepatitis C virus RNA replication occurs on a detergent-resistant membrane that cofractionates with caveolin-2. J. Virol. 77 (7), 4160–4168.
Shirakura, M., Murakami, K., Ichimura, T., Suzuki, R., Shimoji, T., Fukuda, K., Abe, K., Sato, S., Fukasawa, M., Yamakawa, Y., Nishijima, M., Moriishi, K., Matsuura, Y., Wakita, T., Suzuki, T., Howley, P.M., Miyamura, T., Shoji, I., 2007. E6AP ubiquitin ligase mediates ubiquitylation and degradation of hepatitis C virus core protein. J. Virol. 81 (3), 1174–1185.
Suzuki, R., Tamura, K., Li, J., Ishii, K., Matsuura, Y., Miyamura, T., Suzuki, T., 2001. Ubiquitin-mediated degradation of hepatitis C virus core protein is regulated by processing at its carboxyl terminus. Virology 280 (2), 301–309.
Suzuki, T., Ishii, K., Aizaki, H., Wakita, T., 2007. Hepatitis C viral life cycle. Adv. Drug Deliv. Rev. 59 (12), 1200–1212.
Tanaka, T., Inoue, K., Hayashi, Y., Abe, A., Tsukiyama-Kohara, K., Nuriya, H., Aoki, Y., Kawaguchi, R., Kubota, K., Yoshiba, M., Koike, M., Tanaka, S., Kohara, M., 2004. Virological significance of low-level hepatitis B virus infection in patients with hepatitis C virus associated liver disease. J. Med. Virol. 72 (2), 223–229.
Wakita, T., Pietschmann, T., Kato, T., Date, T., Miyamoto, M., Zhao, Z., Murthy, K., Habermann, A., Krausslich, H.G., Mizokami, M., Bartenschlager, R., Liang, T.J., 2005. Production of infectious hepatitis C virus in tissue culture from a cloned viral genome. Nat. Med. 11 (7), 791–796.

JOURNAL OF VIROLOGY, Aug. 2008, p. 7964–7976 Vol. 82, No. 16
0022-538X/08/$08.00+0 doi:10.1128/JVI.00826-08

Interaction of Hepatitis C Virus Nonstructural Protein 5A with Core Protein Is Critical for the Production of Infectious Virus Particles[▽]

Takahiro Masaki,[1] Ryosuke Suzuki,[1] Kyoko Murakami,[1] Hideki Aizaki,[1] Koji Ishii,[1] Asako Murayama,[1] Tomoko Date,[1] Yoshiharu Matsuura,[2] Tatsuo Miyamura,[1] Takaji Wakita,[1] and Tetsuro Suzuki[1]*

Department of Virology II, National Institute of Infectious Diseases, Shinjuku-ku, Tokyo 162-8640, Japan,[1] and Department of Molecular Virology, Research Institute for Microbial Diseases, Osaka University, Suita-shi, Osaka 565-0871, Japan[2]

Received 17 April 2008/Accepted 22 May 2008

Nonstructural protein 5A (NS5A) of the hepatitis C virus (HCV) possesses multiple and diverse functions in RNA replication, interferon resistance, and viral pathogenesis. Recent studies suggest that NS5A is involved in the assembly and maturation of infectious viral particles; however, precisely how NS5A participates in virus production has not been fully elucidated. In the present study, we demonstrate that NS5A is a prerequisite for HCV particle production as a result of its interaction with the viral capsid protein (core protein). The efficiency of virus production correlated well with the levels of interaction between NS5A and the core protein. Alanine substitutions for the C-terminal serine cluster in domain III of NS5A (amino acids 2428, 2430, and 2433) impaired NS5A basal phosphorylation, leading to a marked decrease in NS5A-core interaction, disturbance of the subcellular localization of NS5A, and disruption of virion production. Replacing the same serine cluster with glutamic acid, which mimics the presence of phosphoserines, partially preserved the NS5A-core interaction and virion production, suggesting that phosphorylation of these serine residues is important for virion production. In addition, we found that the alanine substitutions in the serine cluster suppressed the association of the core protein with viral genome RNA, possibly resulting in the inhibition of nucleocapsid assembly. These results suggest that NS5A plays a key role in regulating the early phase of HCV particle formation by interacting with core protein and that its C-terminal serine cluster is a determinant of the NS5A-core interaction.

Hepatitis C virus (HCV) infection is a major public health problem and is prevalent in about 200 million people worldwide (27, 40, 42). Current protocols for treating HCV infection fail to produce a sustained virological response in as many as half of treated individuals, and many cases progress to chronic liver disease, including chronic hepatitis, cirrhosis, and hepatocellular carcinoma (15, 31, 35, 43).

HCV is a positive-strand RNA virus classified in the *Hepacivirus* genus within the *Flaviviridae* family (55). Its approximately 9.6-kb genome is translated into a single polypeptide of about 3,000 amino acids (aa), in which the structural proteins core, E1, and E2 reside in the N-terminal region. A crucial function of core protein is assembly of the viral nucleocapsid. The amino acid sequence of this protein is well conserved among different HCV strains compared to other HCV proteins. The nonstructural (NS) proteins NS3-NS5B are considered to assemble into a membrane-associated HCV RNA replicase complex. NS3 possesses the enzymatic activities of serine protease and RNA helicase, and NS4A serves as a cofactor for NS3 protease. NS4B plays a role in the remodeling of host cell membranes, probably to generate the site for the replicase assembly. NS5B functions as the RNA-dependent RNA polymerase. NS5A is known to play an important but undefined role in viral RNA replication.

NS5A is a phosphoprotein that can be found in basally phosphorylated (56 kDa) and hyperphosphorylated (58 kDa) forms (49). Comparative sequence analyses and limited proteolysis of recombinant NS5A have demonstrated that NS5A is composed of three domains (52). Domain I is relatively conserved among HCV genotypes compared to domains II and III. Analysis of the crystal structure of the conserved domain I that immediately follows the membrane-anchoring α-helix localized at the N terminus revealed a dimeric structure (53). The interface between protein molecules is characterized by a large, basic groove, which has been proposed as a site of RNA binding. In fact, its RNA binding property has been demonstrated biochemically (17). Domains II and III of NS5A are far less understood. Domain II contains a region referred to as the interferon sensitivity determining region, and this region and its C-terminal 26 residues have been shown to be essential for interaction with the interferon-induced, double-stranded RNA-dependent protein kinase (6–10, 38, 39, 48). Domain III includes a number of potential phosphoacceptor sites and is most likely involved in basal phosphorylation. This domain tolerates insertion of large heterologous sequences such as green fluorescent protein (GFP) and is not required for function of NS5A in HCV RNA replication (1, 34). However, a study with the recently established productive HCV cell culture system using genotype 2a isolate JFH-1 (28, 56, 58) demonstrated that while insertion of GFP within the NS5A region does not affect RNA replication, it does produce marked decreases in the production of infectious virus particles (41). This suggests that the C-terminal region of NS5A may affect virus particle production independent of RNA replication. Re-

* Corresponding author. Mailing address: Department of Virology II, National Institute of Infectious Diseases, 1-23-1 Toyama, Shinjuku-ku, Tokyo 162-8640, Japan. Phone: 81 3 5285 1111. Fax: 81 3 5285 1161. E-mail: tesuzuki@nih.go.jp.

▽ Published ahead of print on 4 June 2008.

cently, Miyanari et al. reported that the association of core protein with the NS proteins and replication complexes around lipid droplets (LDs) is critical for producing infectious viruses (33).

In the present study, we demonstrated that NS5A is a prerequisite for HCV particle production via its interaction with core protein, and we identified serine residues in the C-terminal region of NS5A that play an important role in virion production. Substitution of the serine residues with alanine residues inhibited not only the interaction of NS5A with core protein but also HCV RNA-core association and led to a decrease in HCV particle production with no effect on RNA replication.

MATERIALS AND METHODS

DNA construction. Plasmids pJFH1, which contains the full-length JFH-1 cDNA downstream of the T7 RNA promoter sequence, and pSGR-JFH1/Luc, in which the neomycin resistance gene of pSGR-JFH1 has been replaced by the firefly luciferase reporter gene, have been previously described (24, 56). To generate the fluorochrome gene-tagged full-length JFH-1 plasmid, pJFH1/NS5A-GFP, the region encompassing the RsrII site of NS5A and the BsrGI site of NS5B was amplified by PCR, the amplification product was cloned into pGEM-T Easy vector (Promega, Madison, WI), and the resultant plasmid was designated pGEM-JFH1/RsrII-BsrGI. A GFP reporter gene was amplified by PCR from pGreen Lantern-1 (Invitrogen, Carlsbad, CA) with primers containing the XhoI sequence and inserted, after restriction digestion with XhoI, into the XhoI site of pGEM-JFH1/RsrII-BsrGI. The resulting plasmid was digested by RsrII and BsrGI and ligated into pJFH1 similarly digested by RsrII and BsrGI to produce pJFH1/NS5A-GFP. For generation of the fluorochrome gene-tagged subgenomic reporter plasmid, pJFH1/NS5A-GFP was digested by RsrII and SnaBI and ligated into pSGR-JFH1/Luc similarly digested by RsrII and SnaBI. The mutations in the NS5A gene were generated by oligonucleotide-directed mutagenesis (57). To construct plasmids expressing N-terminally FLAG-tagged HCV core protein or hemagglutinin (HA)-tagged NS5A, DNA fragments encoding core protein or NS5A (wild type or mutants) were generated from the full-length JFH-1 cDNA by PCR. The core protein coding sequence, together with a FLAG sequence linked to its N terminus, was cloned into the pCAGGS vector (37). The coding sequences of NS5A, together with an HA sequence linked to their N termini, were also cloned into pCAGGS vectors. All PCR products were confirmed by automated nucleotide sequencing with an ABI Prism 3130 Avant Genetic Analyzer (Applied Biosystems, Tokyo, Japan).

Cells and viruses. The human hepatoma cell line, Huh-7, and JFH1/4-1 cells, which are Huh-7 cells carrying a subgenomic replicon of JFH-1 (32), were maintained in Dulbecco's modified Eagle's medium (DMEM) supplemented with minimal essential medium nonessential amino acids (Invitrogen), 100 units/ml of penicillin, 100 μg/ml of streptomycin, and 10% fetal bovine serum (FBS) at 37°C in a 5% CO_2 incubator. Huh/c-p7 cells, which are Huh-7 cells stably expressing the proteins core to p7 derived from the JFH-1 strain (18), were incubated in DMEM containing 300 μg/ml of zeocin (Invitrogen). HCV particles derived from JFH-1 were produced by transient transfection of Huh-7 cells with in vitro transcribed RNA, as described previously (56, 58). Recombinant vaccinia virus strain DIs, which expresses the bacteriophage T7 RNA polymerase under the control of the vaccinia virus early/late promoter P7.5, was generated and propagated as previously described (19).

DNA transfection, immunoprecipitation (IP), and immunoblotting. For coexpression of FLAG-tagged core protein and HA-tagged NS5A, cells were seeded onto 35-mm wells of a six-well cell culture plate and cultured overnight. Plasmid DNAs (2 μg) were transfected into cells using TransIT-LT1 transfection reagent (Mirus, Madison, WI). Cells were harvested at 48 h posttransfection, washed three times with 1 ml of ice-cold phosphate-buffered saline (PBS), and suspended in 0.25 ml lysis buffer (20 mM Tris-HCl [pH 7.4] containing 135 mM NaCl, 1% Triton X-100, 0.05% sodium dodecyl sulfate [SDS], and 10% glycerol) supplemented with 50 mM NaF, 5 mM Na_3VO_4, 1 μg/ml leupeptin, and 1 mM phenylmethylsulfonyl fluoride (PMSF). Cell lysates were sonicated at 4°C for 5 min, incubated for 30 min at 4°C, and centrifuged at 14,000 × *g* for 5 min at 4°C. After preclearing, the supernatant was immunoprecipitated with 10 μl of anti-FLAG M2-agarose beads (Sigma, St. Louis, MO). For expression of the full-length HCV polyprotein, Huh-7 cells transfected with 10 μg of in vitro transcribed RNAs by electroporation were resuspended in 20 or 30 ml of culture medium, and 10-ml aliquots were seeded into 100-mm culture dishes. At 72 h posttransfection, the cells were incubated in 0.5 ml of lysis buffer (20 mM Tris-HCl [pH 7.4] containing 135 mM NaCl, 1% Triton X-100, 0.5% sodium deoxycholate, and 10% glycerol) supplemented with 50 mM NaF, 5 mM Na_3VO_4, 1 μg/ml leupeptin, and 1 mM PMSF. After preclearing, the supernatant was immunoprecipitated with 5 μg of polyclonal anti-NS5A antibody (34a) or polyclonal anti-C/EBPβ antibody (Santa Cruz Biotechnology, Santa Cruz, CA), and 20 μl of protein G-agarose beads (Invitrogen). The immunocomplex was precipitated with the beads by centrifugation at 800 × *g* for 30 s and then was washed five times with lysis buffer by centrifugation. The proteins binding to the beads were boiled in 20 μl of SDS sample buffer and then subjected to SDS–12.5% polyacrylamide gel electrophoresis (PAGE). The proteins were transferred onto a polyvinylidene difluoride membrane (Immobilon; Millipore, Bedford, MA) and then reacted with a primary antibody and a secondary horseradish peroxidase-conjugated antibody. The immunocomplexes were visualized with an ECL Plus Western Blotting Detection System (GE Healthcare, Buckinghamshire, United Kingdom) and detected using an LAS-3000 imaging analyzer (Fujifilm, Tokyo, Japan).

In vitro synthesis of HCV RNA and RNA transfection. Plasmid DNAs were digested with XbaI and treated with mung bean nuclease (New England Biolabs, Ipswich, MA) to remove the four terminal nucleotides, resulting in the correct 3′ end of the HCV cDNA. Digested DNAs were purified and used as templates for RNA synthesis. HCV RNA was synthesized in vitro using a MEGAscript T7 kit (Ambion, Austin, TX). Synthesized RNA was treated with DNase I (Ambion), followed by acid guanidinium thiocyanate-phenol-chloroform extraction to remove any remaining template DNA. Synthesized HCV RNAs were used for electroporation. Trypsinized Huh-7 cells were washed with Opti-MEM I reduced-serum medium (Invitrogen) and resuspended at 3 × 10^6 cells/ml with Cytomix buffer (54). RNA was mixed with 400 μl of cell suspension and transferred into an electroporation cuvette (Precision Universal Cuvettes; Thermo Hybaid, Middlesex, United Kingdom). Cells were then pulsed at 260 V and 950 μF using a Gene Pulser II unit (Bio-Rad, Hercules, CA). Transfected cells were immediately transferred onto six-well culture plates or 100-mm culture dishes.

Luciferase assay. Cells were harvested at different time points posttransfection of subgenomic reporter replicons and lysed in passive lysis buffer (Promega). The luciferase activity in cells was determined using a luciferase assay system (Promega).

Quantification of HCV core protein. HCV core protein in transfected cells or cell culture supernatants was quantified using a highly sensitive enzyme immunoassay (Ortho HCV antigen ELISA Kit; Ortho Clinical Diagnostics, Tokyo, Japan). To determine intracellular core protein amounts, cell lysates were prepared as described previously (41). To determine the efficiency of core protein release, the ratio of extracellular core protein to total core protein (the sum of intra- and extracellular core protein amounts) was calculated.

Intra- and extracellular infectivity assay. Culture supernatants were harvested 72 h posttransfection, and virus titers were determined by a 50% tissue culture infectious dose ($TCID_{50}$) assay as described previously (28, 46). Virus titration was performed by seeding naive Huh-7 cells in 96-well plates at a density of 1 × 10^4 cells/well. Samples were serially diluted fivefold in complete growth medium and used to infect the seeded cells (six wells per dilution). At 72 h after infection, the inoculated cells were fixed and immunostained with a mouse monoclonal anti-core protein antibody (2H9) (56), followed by an Alexa Fluor 488-conjugated anti-mouse immunoglobulin G (IgG) (Invitrogen). Wells that showed at least one core protein-expressing cell was counted as positive. Cell-associated infectivity was determined essentially as described previously (12, 47). Briefly, cells were extensively washed with PBS, scraped, and centrifuged for 3 min at 120 × *g*. Cell pellets were resuspended in 1 ml of DMEM containing 10% FBS and subjected to four cycles of freezing and thawing using dry ice and a 37°C water bath. Samples were then centrifuged at 2,400 × *g* for 10 min at 4°C to remove cell debris, and cell-associated infectivity was determined by $TCID_{50}$ assay.

Expression of HCV proteins using vaccinia viruses, metabolic labeling of cells, and radioimmunoprecipitation analysis. Metabolic labeling of cells and radioimmunoprecipitation analysis were performed as described by Huang et al. (17) with some modifications. A total of 4 × 10^5 Huh-7 cells were seeded onto each well of six-well cell culture plates and cultured overnight. A 2-μg amount of subgenomic replicon DNAs carrying defined NS5A mutations was transfected into cells using TransIT-LT1 transfection reagent, and at 12 h posttransfection the cells were then infected at a multiplicity of infection of 10 with recombinant vaccinia viruses expressing the T7 RNA polymerase. After 40 h of transfection, cells were incubated in methionine- and cysteine-deficient DMEM (Invitrogen) or phosphate-deficient DMEM (Invitrogen) for 2 h and labeled for 6 h with [^{35}S]methionine and [^{35}S]cysteine (200 μCi/well; GE Healthcare) or

[^{32}P]orthophosphate (250 μCi/well; GE Healthcare). The cells were then washed twice with cold PBS and lysed with SDS lysis buffer (50 mM Tris-HCl [pH 7.6], 0.5% SDS, 1 mM EDTA, 20 μg/ml of PMSF). The cell lysates were passed through a 27-gauge needle several times to shear cellular DNA. After a 10-min incubation at 75°C, the lysates were clarified by centrifugation and diluted five-fold with HNAET buffer (50 mM HEPES [pH 7.5], 150 mM NaCl, 0.67% bovine serum albumin, 1 mM EDTA, 0.33% Triton X-100). After preclearing by incubation with 20 μl of protein G-agarose beads for 1 h at 4°C, the supernatant was incubated with 2 μg of rabbit polyclonal anti-NS5A antibody overnight at 4°C. A 20-μl aliquot of protein G agarose beads was further added and incubated for 2 h at 4°C. The cell pellets were washed three times with 0.5 ml of HNAETS buffer (HNAET containing 0.5% SDS), followed by washing once with 0.5 ml of HNE buffer (50 mM HEPES [pH 7.5], 150 mM NaCl and 1 mM EDTA). After treatment with or without λ protein phosphatase (New England Biolabs), the cell pellets were suspended in 20 μl of SDS sample buffer and boiled for 10 min. The proteins were resolved on 10% SDS-polyacrylamide gels and analyzed by autoradiography.

Subcellular fractionation analysis. All steps were carried out at 4°C in the presence of a protease inhibitor cocktail (Complete; Roche, Mannheim, Germany) as described previously (20), with some modifications. Cells were suspended in four cell volumes of homogenization buffer (50 mM NaCl, 10 mM triethylamine [pH 7.4], 1 mM EDTA), snap frozen in liquid nitrogen, stored at −80°C, and thawed in a water bath at room temperature. Supernatants (0.4 ml) were layered on linear 10-ml iodixanol gradients from 2.5 to 25% and centrifuged at 37,000 rpm for 3.5 h in an SW41 rotor (Beckman, Fullerton, CA), followed by collection of 0.8-ml fractions from the top. Each fraction was concentrated by Centricon YM30 (Millipore), separated by SDS-PAGE, and immunoblotted with a rabbit polyclonal anti-calnexin antibody (Stressgen Biotechnologies, Victoria, Canada), a mouse monoclonal anti-adipose differentiation-related protein (ADRP) antibody (Progen Biotechnik, Heidelberg, Germany), or a rabbit polyclonal anti-NS5A antibody. The core protein amount in each fraction was also determined by enzyme-linked immunosorbent assay (ELISA).

IP-RT-PCR. The process of cell lysis to RNA purification was carried out essentially as described by Johnson et al. (21) with some modifications. A total of 3×10^6 Huh-7 cells were transfected with 10 μg of in vitro transcribed HCV RNAs and resuspended in 20 or 30 ml of culture medium, after which 10-ml aliquots were seeded into 100-mm culture dishes. At 72 h posttransfection, the cells were scraped and incubated in 500 μl of hypotonic buffer (10 mM HEPES [pH 7.6], 1.5 mM $MgCl_2$, 10 mM KCl, 0.2 mM PMSF) per dish. The cells were passed through a 20-gauge needle several times, lysed with Nonidet P-40 at a final concentration of 1%, and incubated on ice for an additional 10 min. After centrifugation at 4,000 × *g* at 4°C for 15 min, glycerol was added to the supernatants at a final concentration of 5%. The cell lysates were incubated with 20 μl of protein G-agarose beads for 30 min at room temperature. After the cell lysates were removed from protein G-agarose beads, 5 μg of mouse monoclonal anti-core protein antibody or normal mouse IgG (Sigma) as a negative control was added, and samples were incubated for an additional 1 h at room temperature. A 20-μl aliquot of protein G-agarose beads per sample was added to the cell lysates and incubated for 1 h. After incubation, the beads were washed three times with wash buffer (10 mM Tris-HCl [pH 7.6], 100 mM KCl, 5 mM $MgCl_2$, and 1 mM dithiothreitol) and eluted in 100 μl of elution buffer (50 mM Tris-HCl [pH 8.0], 1% SDS, and 10 mM EDTA) at 65°C for 10 min. After treatment with 100 μg of proteinase K at 37°C for 30 min, the RNAs in immunocomplexes were isolated by acid guanidinium thiocyanate-phenol-chloroform extraction. Reverse transcriptase PCR (RT-PCR) was carried out using random hexamer and Superscript II RT (Invitrogen), followed by nested PCR with LA *Taq* DNA polymerase (TaKaRa, Shiga, Japan) and primer sets amplifying the fragments of nucleotides (nt) 129 to 2367 and nt 7267 to 9463 of the JFH-1 genome. To amplify the fragment of nt 129 to 2367, the sense primer 5′-CTGTGAGGAACTACTGTCTT-3′ and the antisense primer 5′-TCCACGATGTTCTGGTGAAG-3′ were used for first-round PCR; the sense primer 5′-CGGGAGAGCCATAGTGG-3′ and the antisense primer 5′-CATTCCGTGGTAGAGTGCA-3′ were used for second-round PCR. To amplify the fragment of nt 7267 to 9463, the sense primer 5′-GTCCAGGGTGCCCGTTCTGGACT-3′ and the antisense primer 5′-GCGGCTCACGGACCTTTCAC-3′ were used for first-round PCR; the sense primer 5′-CACCGTTGCTGGTTGTGCT-3′ and the antisense primer 5′-GTGTACCTAGTGTGTGCCGCTCTA-3′ were used for second-round PCR.

Indirect immunofluorescence analysis. Cells incubated for 3 days after transfection with JFH-1 RNAs were seeded in an eight-well chamber slide (BD Biosciences, San Jose, CA) and cultured overnight. The adherent cells were washed twice with PBS and fixed with 4% paraformaldehyde at room temperature. After a washing step with PBS, the cells were permeabilized with PBS containing 0.3% Triton X-100 and 2% FBS for 1 h at room temperature and stained with a rabbit polyclonal anti-NS5A antibody and a mouse monoclonal anti-core protein antibody. The fluorescent secondary antibodies were Alexa Fluor 488- or Alexa Fluor 555-conjugated anti-rabbit or anti-mouse IgG antibodies (Invitrogen). Analyses of JFH-1 were performed on a Zeiss confocal laser scanning microscope LSM 510 (Carl Zeiss, Oberkochen, Germany).

RESULTS

Mutations of serine residues at the NS5A C terminus impair basal phosphorylation but have little effect on viral RNA replication. As demonstrated in a previous study, insertion of GFP into the NS5A C terminus does not significantly affect viral RNA replication but reduces the generation of infectious HCV particles (41). The C-terminal region of NS5A contains highly conserved serine residues that are involved in basal phosphorylation (1, 23, 49). To examine the involvement of the serine clusters (cluster 3-A [CL3A] and cluster 3-B [CL3B]) in the C-terminal region of NS5A in HCV particle production, we created mutated HCV genomes as well as subgenomic replicons carrying alanine substitutions for the conserved serine residues at aa 2384, 2388, 2390, and 2391 (residues are numbered according to the positions within the original JFH-1 polyprotein) (CL3A/SA); at aa 2428, 2430, and 2433 (CL3B/SA); or an in-frame deletion spanning aa 2384 to 2433 (Δ2384–2433) (Fig. 1). A construct with an in-frame insertion of GFP (NS5A-GFP) was also generated as described previously for the Con1 isolate (34).

First, we analyzed the effects of the NS5A mutations on HCV RNA replication using a transient RNA replication assay using subgenomic luciferase reporter replicons (Fig. 2A) and found that the serine-to-alanine substitutions (CL3A/SA and CL3B/SA) did not affect viral RNA replication. NS5A-GFP and Δ2384–2433 slightly reduced RNA replication, indicating that the mutations of the NS5A C terminus tested in this study do not critically affect RNA replication, which is consistent with previous reports (1, 34, 51).

Next, the phosphorylation status of the mutated NS5A was analyzed as described in Materials and Methods (Fig. 2B). NS5A was isolated from radiolabeled cells by IP and analyzed either directly by SDS-PAGE or after treatment with λ protein phosphatase. Analysis of ^{32}P-radiolabeled proteins revealed that the CL3A/SA, CL3B/SA, and Δ2384–2433 mutations resulted in marked reduction of basal phosphorylation (Fig. 2B, compare lane 1 with lanes 3, 5, and 7 in the top panel). All ^{32}P-labeled NS5A proteins were sensitive to treatment with phosphatase (lanes 2, 4, 6, and 8). The possibility that loss of signal after dephosphorylation was due to contaminating proteases present in the phosphatase preparations can be ruled out because no degradation of the ^{35}S-labeled proteins was observed (Fig. 2B, bottom panel). These results suggest that mutations in the C-terminal serine cluster of NS5A impair basal phosphorylation but have no significant effect on viral RNA replication.

Effect of mutations introduced into the NS5A C terminus on the production of infectious HCV particles. To analyze HCV particle production from cells transfected with the in vitro transcribed viral genomic RNAs, we harvested supernatants and cells at 4, 24, 48, 72, and 96 h posttransfection and measured the amounts of core protein. As shown in Fig. 3A, comparable amounts of core proteins were detected in all transfected cells 4 h after transfection, reflecting unchanged